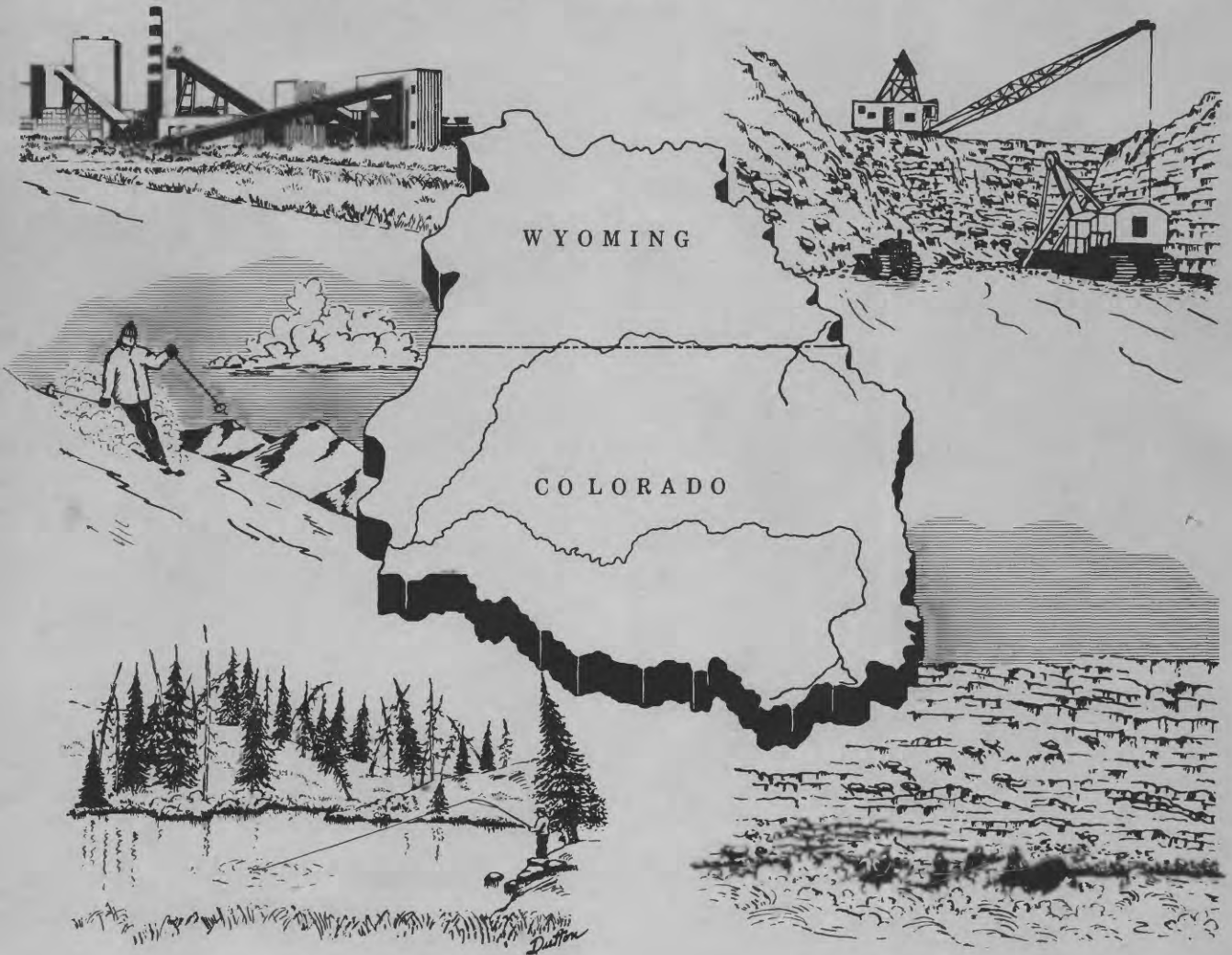




UNITED STATES
DEPARTMENT OF THE INTERIOR
GEOLOGICAL SURVEY

PRELIMINARY APPLICATIONS OF LANDSAT IMAGES AND AERIAL PHOTOGRAPHY FOR DETERMINING LAND-USE, GEOLOGIC, AND HYDROLOGIC CHARACTERISTICS-- YAMPA RIVER BASIN, COLORADO AND WYOMING



PRELIMINARY APPLICATIONS OF LANDSAT IMAGES AND AERIAL PHOTOGRAPHY
FOR DETERMINING LAND-USE, GEOLOGIC, AND HYDROLOGIC
CHARACTERISTICS--YAMPA RIVER BASIN, COLORADO AND WYOMING
By Frederick J. Heimes, Gerald K. Moore, and Timothy Doak Steele

U.S. GEOLOGICAL SURVEY

Water-Resources Investigations 78-96



Open-File Report

October 1978

U.S. DEPARTMENT OF THE INTERIOR

CECIL D. ANDRUS, Secretary

GEOLOGICAL SURVEY

H. William Menard, Director

Open-File Report

For additional information write to:

District Chief
U.S. Geological Survey
Box 25046, Mail Stop 415
Denver Federal Center
Lakewood, CO 80225

CONTENTS

	Page
Glossary	V
Metric conversion table	V
Abstract	1
Introduction	2
Remote-sensing data and analysis techniques	2
Data	2
Analysis techniques	7
Applications	7
Land-use classification	7
Lineament mapping	28
Mapping areal snow-cover extent	30
Turbidity estimation	33
Future considerations	39
References	41
Supplemental information	43
Landsat system	43
Photographic-interpretation and digital-analysis techniques and equipment	45
Photographic interpretation	45
Digital-analysis techniques	45
Digital-image-processing equipment	47

ILLUSTRATIONS

Figure 1. Map of the Yampa River basin, Colorado and Wyoming	3
2. Map showing approximate areal coverage of Landsat images used for analysis	5
3. Map showing aerial-photography flight-line coverage of the southern Yampa River basin, May 31, 1977	6
4. Part of color-composite image of Landsat scene 5127-16532, August 24, 1975	11
5. Part of black-and-white image, band 7, of Landsat scene 1947-17030, February 25, 1975	13
6. Selected parts of the August 24, 1975, Landsat image chosen for detailed study	15
7. Enlarged part of August 24, 1975, Landsat image (fig. 6) with training sets for irrigated hay-meadow class outlined	16
8. Image-100 land-use classification of the Hayden Powerplant area	18
9. Enlarged part of the August 24, 1975, Landsat image with four areas outlined	19
10. Enlargement of area 2 (fig. 9) with training sets for water and rangeland classes outlined	21

CONTENTS

	Page
Figure 11. Two-dimensional plot of spectral distribution within and between initial land-use and land-cover classes using Landsat bands 5 and 7	23
12. Two-dimensional plot of spectral distribution within and between final land-use and land-cover classes using Landsat bands 5 and 7	24
13. Part of a Landsat image showing land-use classification of the region along the Yampa River from confluence of Elkhead Creek to just west of Streamboat Springs.	26
14. Part of black-and-white image, band 7, of Landsat scene 1948-17084, February 26, 1975	29
15. Lineament and fault map superimposed on Landsat scene 1948-17084, February 26, 1975.	31
16. Snow-cover classification of Yampa River basin part of the February 26, 1975, Landsat image.	34
17. Map showing locations of sampling sites for the turbidity/spectral-reflectance investigation.	36
18. Graph showing mean digital reflected-energy values versus turbidity values for the three spectral bands (layers): Blue, green, and red.	38
19. Sketches showing: <i>A</i> , Landsat configuration; and <i>B</i> , Multi-spectral scanner system scanning arrangement.	44

TABLES

Table 1. Camera and film specifications, May 31, 1977; U-2 overflight.	4
2. Land-use and land-cover classification system for use with remote-sensor data.	9
3. Initial land-use and land-cover classes selected for classification using the Interactive Digital Image Manipulation System	22
4. Final land-use and land-cover classes selected for classification using the Interactive Digital Image Manipulation System	25
5. Turbidity and suspended-sediment measurements obtained May 31 and June 1, 1977	35
6. Digital reflected-energy values and associated statistics calculated from analysis of color transparencies.	37
7. Regression equations and associated statistics developed for prediction of turbidity	39

GLOSSARY

- color-composite image*.--A color image produced by assigning primary colors to three spectral bands. For Landsat images, blue ordinarily is assigned to band 4 (0.5-0.6 micrometer), green to band 5 (0.6-0.7 micrometer), and red to band 7 (0.8-1.1 micrometers), forming an image closely approximating a color-infrared photograph.
- ground information*.--Term used for data and information obtained by ground-based reconnaissance which can be used to check and confirm interpretations of remotely-sensed data.
- multispectral scanner (MSS)*.--A remote-sensing device which senses data in two or more discrete spectral bands. In Landsat, the sensor scans the ground using an oscillating plane mirror in a path normal to the satellite's path.
- pixel*.--An acronym for picture element (resolution cell). In reference to Landsat data, the term refers to the area on the ground (185×260 feet or 56×79 meters) that is viewed by the multispectral scanner at each point that the signal is sampled.
- pixel value*.--Digital value of reflected energy from a surface area represented by a given pixel.
- remote sensing*.--The measurement or acquisition of information pertaining to some property of an object or phenomenon, by use of a sensing device that is not in physical contact with the object or phenomenon under study.
- spectral band*.--An interval in the electromagnetic spectrum defined by wavelengths, frequencies, or wave numbers.
- spectral signature*.--Quantitative measurement of the electromagnetic properties of an object at one or several wavelength intervals.
- sun synchronous*.--An earth-satellite orbit in which the orbital plane is near polar and the altitude is such that the satellite passes over all places on the earth having the same latitude twice daily at nearly the same local sun time.

METRIC CONVERSION TABLE

The inch-pound units used in this report may be converted to metric units by using the following conversion factors:

<i>Multiply inch-pound unit</i>	<i>By</i>	<i>To obtain metric unit</i>
inch (in.)	25.4	millimeter (mm)
	2.54×10^4	micrometer (μm)
foot (ft)	0.3048	meter (m)
mile (mi)	1.609	kilometer (km)
square mile (mi ²)	2.590	square kilometer (km ²)
acre	0.4047	hectare (ha)

PRELIMINARY APPLICATIONS OF LANDSAT IMAGES AND AERIAL PHOTOGRAPHY
FOR DETERMINING LAND-USE, GEOLOGIC, AND HYDROLOGIC
CHARACTERISTICS--YAMPA RIVER BASIN, COLORADO AND WYOMING

By Frederick J. Heimes, Gerald K. Moore, and Timothy Doak Steele

ABSTRACT

Expanded energy- and recreation-related activities in the Yampa River basin, Colorado and Wyoming, have caused a rapid increase in economic development which will result in increased demand and competition for natural resources. Remote-sensing data may provide timely information which is required in planning for efficient allocation of the basin's natural resources. This study used Landsat images and small-scale color and color-infrared photographs for selected geologic, hydrologic, and land-use applications within the Yampa River basin.

Applications of Landsat data included: (1) Regional land-use classification, (2) lineament mapping, and (3) areal snow-cover mapping. Results from the Landsat investigations indicated that: (1) Regional land-cover classification determined from Landsat data compared favorably with land use defined from aerial photographs and available ground information, (2) numerous lineaments that may be indicators of potential ground-water resources were mapped from images using photointerpretation techniques, and (3) snow cover could generally be mapped for large areas with the exception of some densely forested areas of the basin and areas having a large percentage of winter-season cloud cover. The analysis of Landsat data tended to be qualitative for the most part, because of a lack of sufficient and timely ground information to quantitatively evaluate their accuracy.

Aerial photographs were used for estimating turbidity at eight locations on three streams in the basin. Spectral reflectance values obtained by digitizing photographs were compared with measured turbidity values. Results showed correlations (variances explained of greater than 90 percent) between spectral reflectance obtained from color photographs and measured turbidity values.

Results from these preliminary investigations will be incorporated in the design of continuing studies which will further evaluate the techniques employed and provide more quantitative measures of their accuracy.

INTRODUCTION

The Yampa River basin, encompassing an area of approximately 8,080 mi² (21,000 km²), is located in northwestern Colorado and south-central Wyoming (fig. 1). This region currently is undergoing rapid economic development primarily as a result of expanded energy-related activities, principally mining and transport of coal and conversion of coal to electrical power and possibly gas products. Additionally, the eastern part of the Yampa River basin, especially in the area of Steamboat Springs, Colo. (fig. 1), has experienced a rapid growth in recreational activity. This results in large seasonal influxes of people. The current (1977) year-round basin population is approximately 20,000. The rapid increase in energy- and recreation-related activities is resulting in an increased demand and subsequent competition for natural resources in this region. Effective planning for optimal allocation of these natural resources requires the collection and analysis of large amounts of diverse data on a timely basis.

The purpose of this study was to determine the potential of selected remote-sensing applications for providing some of these timely regional-level data which could be used in conjunction with other data collected by conventional methods. Landsat (land satellite) images and 1:100,000-scale color and color-infrared aerial photographs were used in four selected remote-sensing applications. Landsat images were used in the following applications: (1) Regional land-use classification, (2) lineament mapping, and (3) areal snow-cover mapping. The color and color-infrared aerial photographs were used for estimating turbidity in selected streams in the basin.

The investigations conducted using these four applications were designed as preliminary evaluations of the feasibility of these approaches and were not oriented toward the development of operational procedures. However, it is hoped that the results from this and subsequent studies will eventually lead to operational techniques using remote-sensing technology. Such techniques would facilitate the rapid collection and analysis of some of the data required for efficient allocation of resources on a regional basis.

This study was conducted as part of the Yampa River basin assessment (Steele and others, 1976). The basin-assessment project is a 2½-year program designed to determine the availability and quality of the water resources and to evaluate the potential environmental and socioeconomic impacts of coal-resource development within the basin.

REMOTE-SENSING DATA AND ANALYSIS TECHNIQUES

Data

This section lists the types and sources of remote-sensing data that were used in the study and briefly discusses the general analytical techniques that were used. More detailed descriptions of the Landsat system, image processing systems, and techniques that were employed in analyzing the

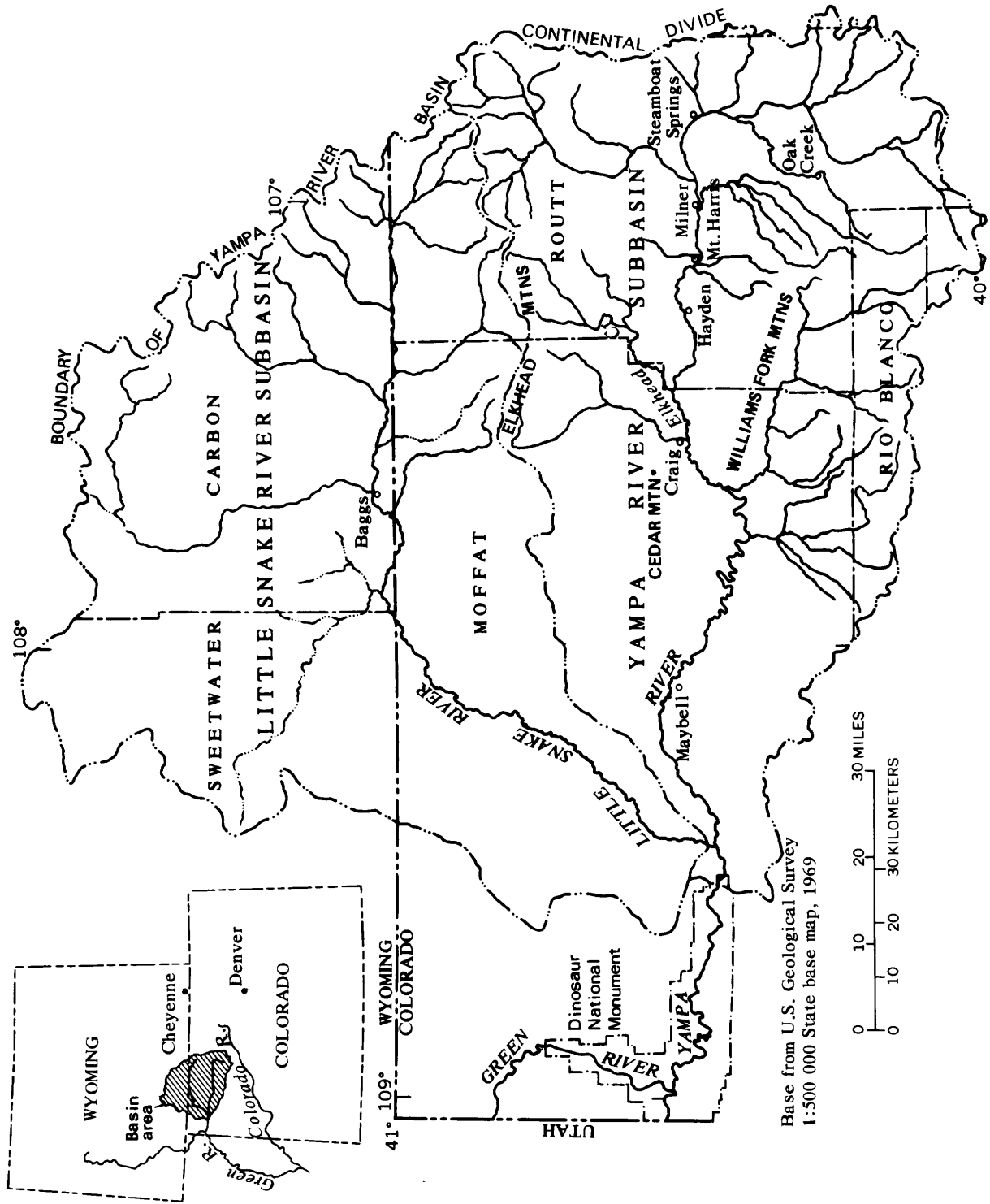


Figure 1.--The Yampa River basin, Colorado and Wyoming.

remote-sensing data are contained in the Supplemental Information section of this report.

Multispectral-scanner (MSS) data were selected for use in the Landsat applications. Three images encompassing the general area of northwestern Colorado were selected for analysis (fig. 2). The dates of acquisition and scene-identification numbers of the images are as follows:

1. February 25, 1975, Scene 1947-17030.
2. February 26, 1975, Scene 1948-17084.
3. August 24, 1975, Scene 5127-16532.

The images for February 25 and August 24 encompass the same geographical region which includes the eastern part of the Yampa River basin. The image for February 26 includes most of the western part of the basin.

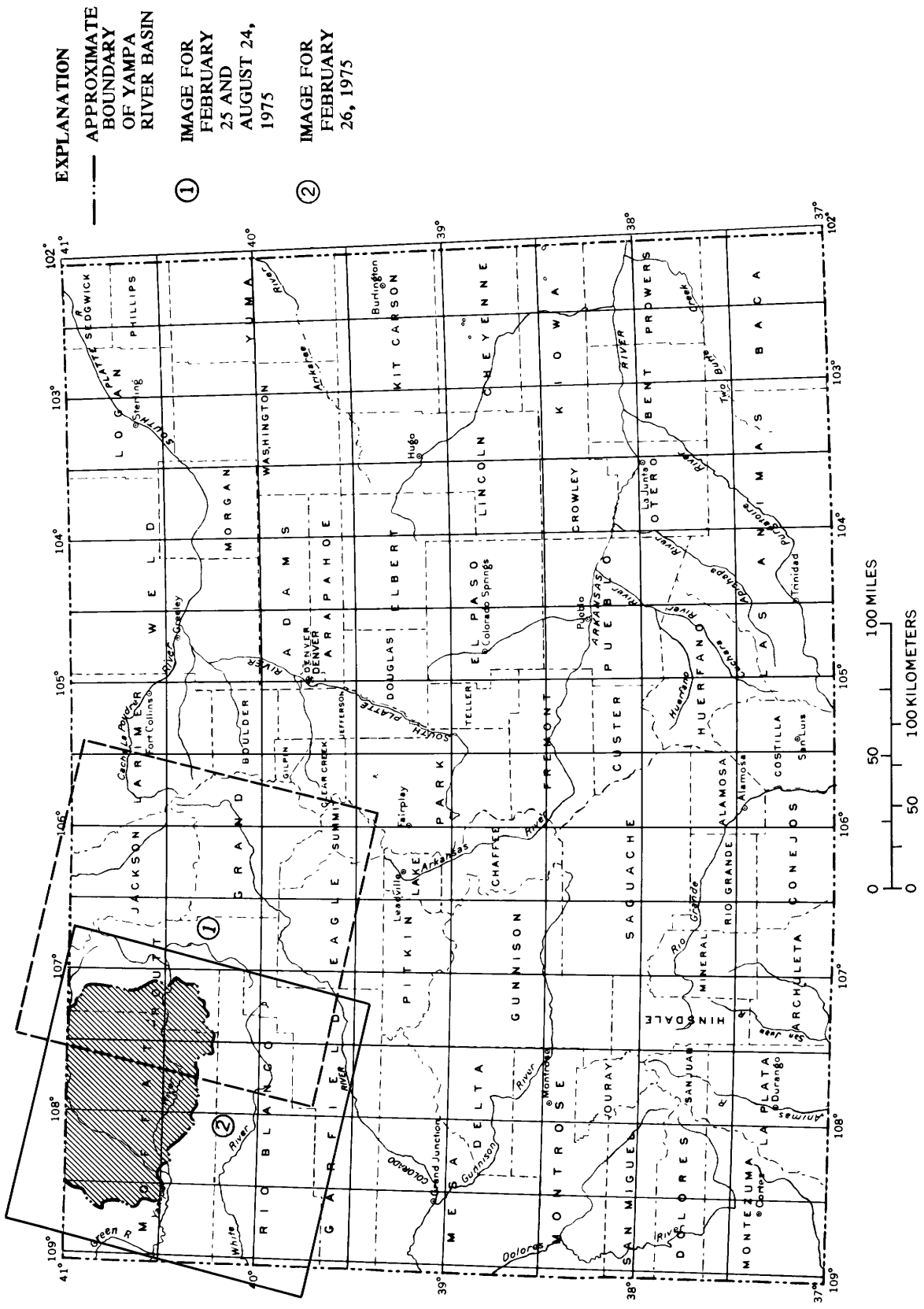
Data for the three images included: (1) Computer-compatible digital tapes of the February 26 and August 24, 1975, images; (2) color-composite 1:1,000,000-scale photographs of the August 24, 1975, image; and (3) band-7 black-and-white 1:1,000,000-scale photographs of the February 25 and 26, 1975, images. The main rationale for selection of 1975 Landsat images was the fact that good quality imagery for both summer and winter seasons existed and that digital tapes for the images were available at the U.S. Geological Survey's EROS Data Center in Sioux Falls, S. Dak.

Aerial photographs, scale 1:100,000, taken by the National Aeronautics and Space Administration's U-2 aircraft were used in the investigation of turbidity. The photographs used in this investigation were selected from photography acquired on May 31, 1977, which included the part of the Yampa River basin south of lat 40°37' (fig. 3). Color and color-infrared positive transparency films were used for the analysis. Detailed information about the camera systems used and the film characteristics are summarized in table 1.

Table 1.--*Camera and film specifications, May 31, 1977; U-2 overflight*

[Data adapted from National Aeronautics and Space Administration, flight summary 77-067, 1977]

	Camera 1	Camera 2
Sensor type----	Wild RC-10-----	Wild RC-10.
Focal length---	6 inches (153.21 mm)-----	6 inches (153.05 mm).
Film type-----	High-definition aerochrome infrared, S0-127.	Aerial color, S0-242.
Filtration-----	CC 0.05C+0.058+2.2AV-----	2.2AV.
Spectral band--	0.51-0.90 micrometer-----	0.40-0.70 micrometer.
F stop-----	4.0-----	4.0.
Shutter speed--	1/100 second-----	1/100 second.



EXPLANATION

--- APPROXIMATE BOUNDARY OF YAMPA RIVER BASIN

①

IMAGE FOR FEBRUARY 25 AND AUGUST 24, 1975

②

IMAGE FOR FEBRUARY 26, 1975

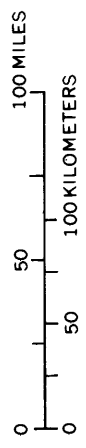


Figure 2.---Approximate areal coverage of Landsat images used for analysis.

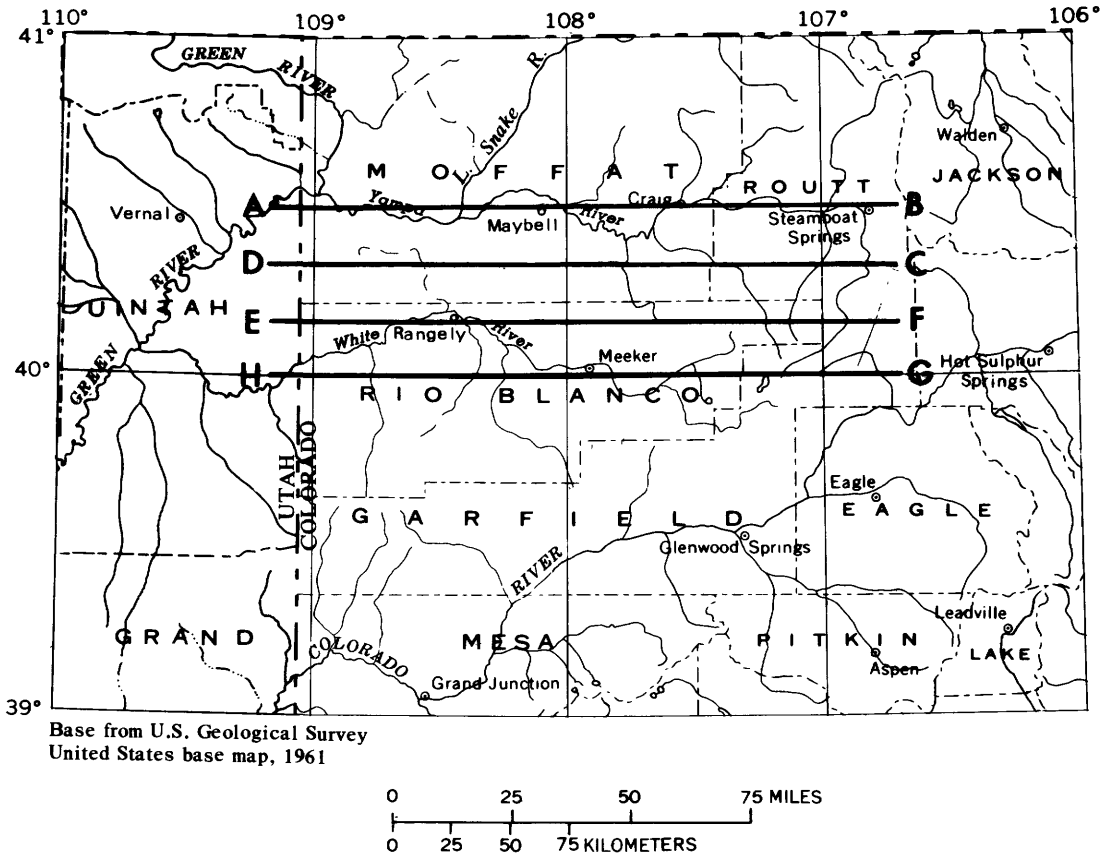


Figure 3.-- Aerial-photography flight-line coverage of the southern Yampa River basin, May 31, 1977.

Several other forms of support information were used in the study; they included (1) topographic maps, (2) 1:24,000-scale black-and-white and color-infrared aerial photographs, and (3) ground reconnaissance and sampling. The specific uses of the data listed here will be included in the discussion of each of the individual remote-sensing applications.

Analysis Techniques

Two techniques were used in the analysis of Landsat data and aerial photographs--photographic interpretation and digital-image processing. Photographic-interpretation techniques (p.45) were used in two phases of analysis. In the first phase, photographic interpretation of the 1:24,000-scale black-and-white and color-infrared photographs was used in conjunction with ground information to: (1) Locate and identify surface features for use in defining training sets for supervised classification techniques (p. 46), and (2) to provide information for subsequent evaluation of Landsat classification results. In the second phase, photographic-interpretation techniques were used directly in the analysis and classification of Landsat images. Digital-image processing (p. 45) for analysis and classification was applied to: (1) Landsat digital data, and (2) digitized 1:100,000-scale color and color-infrared photographs. Digital-image processing was conducted using the Image-100 System¹ and Interactive Digital Image Manipulation System (IDIMS) (p. 47).

APPLICATIONS

Land-Use Classification

Large variations in altitude (5,000-12,000 ft or 1,500-3,700 m) and precipitation (9-50 in. or 230-1,300 mm) produce a wide range of land-use categories in the Yampa River basin. Timber harvesting and grazing represent the largest areal land use; 89 percent of the basin's area is devoted to these activities (Colorado Water Conservation Board and U.S. Department of Agriculture, 1969). Despite the lesser areas involved, farming and energy-resource development are major contributors to the regional economy (Udis and Hess, 1976). In some areas, agricultural land-use patterns tend to shift back and forth between grazing and dryland farming of small grains in response to prices in the wholesale market. The type of land use and the land-reclamation and conservation practices used can have a pronounced effect on the amount of soil erosion that occurs in a given area. This is especially true for many of the areas of dryland farming and surface mining of coal in the Yampa River basin (Routt County Soil Conservation District, 1977). These areas are potential contributors of considerable quantities of sediments to the streams that drain them. Unsound grazing and timber-management practices also could result in relatively large erosion rates in certain areas.

¹The use of trade names in this report is for identification only and does not imply endorsement by the U.S. Geological Survey.

Current methods of collecting and updating information on land-use practices frequently are costly and time consuming. This is especially true for a large region like the Yampa River basin where land use is diverse and often subject to change both at regular and irregular intervals. A dynamic system such as this requires regular updates of information if the information is to be a realistic tool for planning and subsequent development and allocations of regional natural resources.

Landsat images may be a source of data to assist in determining land use and monitoring its changes. Landsat provides repetitive coverage of large areas which may be suitable for determining land-use categories on a regional scale and updating the information at regular intervals. A number of studies have been conducted that use Landsat data for land-use classification. These studies have resulted in varying degrees of success. However, few studies applying Landsat data to land-use classification have been conducted in regions that are as complex and diverse both culturally and physically as the Yampa River basin. The Yampa River basin is representative of several regions in the Rocky Mountains which are undergoing rapid development of energy resources. The basin's complexity, diversity, and potential for rapid development make it a challenging area for testing the feasibility of using Landsat data for land-use classification.

Both photographic-interpretation and digital-image processing techniques were used for land-use classification. Photographic-interpretation techniques were applied to band-7 black-and-white photographs of Landsat images for February 25 and 26, 1975, and to a color-composite photograph of the Landsat image for August 24, 1975. Image scales of 1:1,000,000 were used in this analysis. Computer-compatible digital tapes of the Landsat image for August 24, 1975, were used for digital-image processing and analysis.

Digital-image processing and analysis techniques were emphasized in land-use applications primarily because of their ability to classify large areas much more rapidly than photographic-interpretation methods. Therefore, photographic-interpretation techniques were used only for identification of land-use features that would be difficult to identify by spectral characteristics (digital analysis) alone and which would be relatively easy to identify by incorporation of spatial characteristics, such as linearity.

The land-use classification system suggested by Anderson, Hardy, Roach, and Witmer (1976) was used as a guide in the definition of possible land-use categories (table 2). Also, results from the Landsat classification were compared with table 2 to determine the level of classification that could be obtained, for various categories, using digital-image processing.

Land-use categories and representative areas (training sets) for each category were defined using a combination of black-and-white 1:24,000-scale aerial photographs and available ground information. The black-and-white aerial photographs obtained in 1973 were the most recent available coverage of the area at the time of the analysis. This proved to be somewhat of a disadvantage in selection of land-use categories and representative training-set areas on the 1975 Landsat imagery. However, sufficient sites representing

Table 2.--*Land-use and land-cover classification system for use with remote-sensor data*

[Modified from Anderson, Hardy, Roach, and Witmer, 1976]

Category number	Level I	Level II
1	Urban or built-up land--	1.1 Residential.
		1.2 Commercial and services.
		1.3 Industrial.
		1.4 Transportation, communications, and utilities.
		1.5 Industrial and commercial complexes.
		1.6 Mixed urban or built-up land.
		1.7 Other urban or built-up land.
2	Agricultural land-----	2.1 Cropland and pasture.
		2.2 Orchards, groves, vineyards, nurseries, and ornamental horticultural areas.
		2.3 Confined feeding operations.
		2.4 Other agricultural land.
3	Rangeland-----	3.1 Herbaceous rangeland.
		3.2 Shrub and brush rangeland.
		3.3 Mixed rangeland.
4	Forest land-----	4.1 Deciduous forest land.
		4.2 Evergreen forest land.
		4.3 Mixed forest land.
5	Water-----	5.1 Streams and canals.
		5.2 Lakes.
		5.3 Reservoirs.
		5.4 Bays and estuaries.
6	Wetland-----	6.1 Forested wetland.
		6.2 Nonforested wetland.
7	Barren land-----	7.1 Dry salt flats.
		7.2 Beaches.
		7.3 Sandy areas other than beaches.
		7.4 Bare, exposed rock.
		7.5 Strip mines, quarries, and gravel pits.
		7.6 Transitional areas.
		7.7 Mixed barren land.
8	Tundra-----	8.1 Shrub and brush tundra.
		8.2 Herbaceous tundra.
		8.3 Bare ground tundra.
		8.4 Wet tundra.
		8.5 Mixed tundra.
9	Perennial snow or ice---	9.1 Perennial snowfields.
		9.2 Glaciers.

the variety of land-use categories present were defined by comparing the 1973 photographs with updated ground information to locate areas that remained virtually unchanged between 1973 and 1975.

Selection of the best Landsat MSS-band configuration for analysis of a certain surface feature of interest is a function of many factors, including the type of feature to be evaluated, the time of year, the atmospheric conditions, and the quality of the imagery. Color-composite images (see Glossary) tend to enhance the various features displayed on the imagery. Color-composite images generally provide photointerpreters with more usable information for the majority of applications than is available from single-band black-and-white images.

For example, on the August 24, 1975, image (fig. 4), selected features appear as follows:

1. Clouds--white with a corresponding shadow on the northwest side.
2. Snow--white, but with no shadow.
3. Water--black.
4. Irrigated or lush vegetation--bright pink or red.
5. Dryland agriculture--brown and green areas with defined patterns.
6. Rangeland--blue or green with no defined patterns.
7. Sparse vegetation (barren land)--shades varying from blue or gray to almost white.
8. Conifers--dark red or brown to almost black.
9. Deciduous vegetation--various shades of red.

The following land-use categories were selected for determination by photographic-interpretation techniques:

<i>Level I</i>	<i>Level II</i>
Urban-----	Residential and commercial.
	Transportation and utilities.
Barren land---	Strip mines.

Urban areas in the Yampa River basin are small. The largest towns in the basin are Craig and Steamboat Springs in Colorado (fig. 1). Estimated populations in 1975 were 8,000 for Craig and 5,900 for Steamboat Springs. A snow-covered image is generally best for determining locations of urban centers and major highways because of the contrast between the snow and the

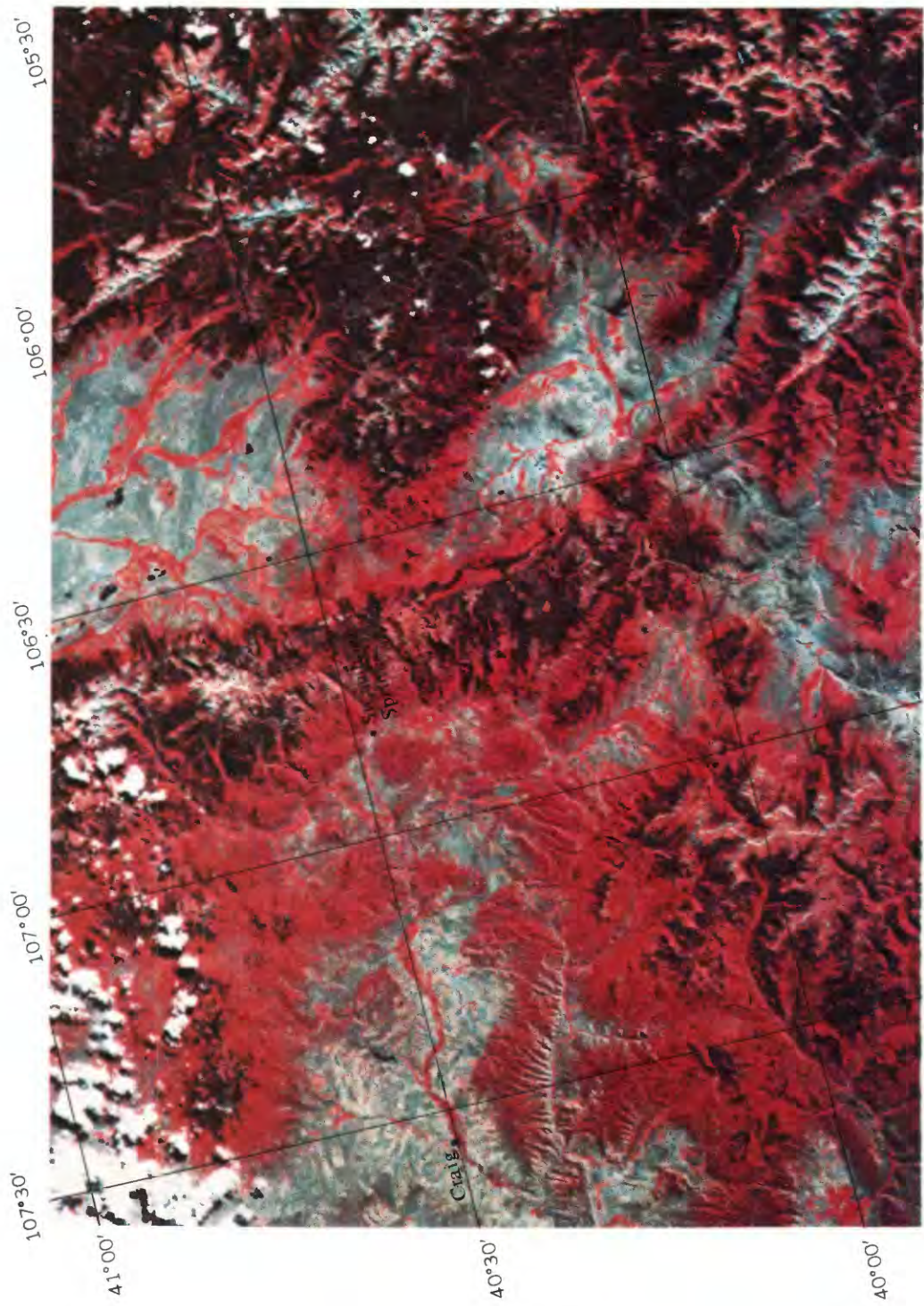


Figure 4.-- Part of color-composite image of Landsat scene 5127-16532, August 24, 1975.

snowplowed traffic areas. Despite the relatively small size of the communities, Craig and Steamboat Springs were easily identified on the Landsat image for February 25, 1975 (fig. 5). Smaller communities, such as Hayden, Colo. (estimated population of about 1,800 in 1975), could be identified on the image with prior information on their location. U.S. Highway 40, the major two-lane east-west highway in the basin, is visible except in areas shaded by steep relief. Although the highway has a pavement width less than the resolution of a pixel (see Glossary), it is visible because of its extended linear trend and its contrast with surrounding snow cover. With high contrast conditions, extended linear features as small as 50 ft (15 m) wide may be detected (Wiedel and Kleckner, 1974). Other paved highways in the basin can be identified only in segments, because they have less traffic or may be shaded by adjacent steep relief.

A combination of the band-7 black-and-white image for February 25, 1975, and the color-composite image for August 24, 1975, was used to locate active surface mines. Surface mines in the basin are difficult to find on the images without prior information regarding their general location. However, once located on the images, active mined areas generally can be delineated and their areal extent determined. Active mines appear dark on the winter black-and-white photograph, contrasting with the surrounding snow. On summer color-composite images, active surface mines are characterized by a combination of hue (blue gray to black) and sometimes distinctive spatial characteristics. Older abandoned and unreclaimed surface mines were very difficult to locate on the satellite imagery in most instances. This was because rangeland vegetation had established itself on the mine spoils, giving these areas spectral characteristics similar to sparsely vegetated rangeland. The small-scale resolution of the Landsat MSS (see Glossary) is generally not sufficient to depict the lined-row characteristic of the unreclaimed spoils once natural vegetation has begun to establish itself on them. Most of the present and past surface-mining operations in the Yampa River basin are located in areas of a mixed rangeland category of land use so that they contrast much less with surrounding areas than do mines located in forested regions. Also, unlike eastern surface-mining operations, individual strips do not follow the terrain contours, which tend to make them less distinctive on Landsat images.

Analysis by digital-image processing was conducted using both the Image-100 System and IDIMS. Both systems were selected because each contained different classification functions (p. 48) which afforded the opportunity to maximize the number of analysis techniques that could be evaluated for land-use classifications.

The August 24, 1975, Landsat image was selected for digital analysis to determine land-use classes. The emphasis was on determining the categories of land use that could be identified by this method and the level of classification (table 2) that was possible within each of the categories. Comparison of several different classification functions allowed evaluation of the relative merits of each of the functions for land-use classification and mapping.



Figure 5.-- Part of black-and-white image, band 7, of Landsat scene 1947-17030, February 25, 1975.

The fast data-processing and analysis functions of the Image-100 System were used advantageously for a number of tasks. The entire Landsat image was examined and parts of the image were selected for detailed study (fig. 6). The selected parts were enhanced to improve interpretability by contrast stretching; that is, the contrast between features and their surroundings was enhanced. A color-composite image of data from three spectral bands was displayed. Filter colors and gain-and-bias controls on the Image 100 were adjusted to enhance selected features of interest.

Classification was accomplished using the parallelepiped supervised technique (p. 46). For this approach, a data group which was considered to be representative of a land-use category was selected as a training set. Several areas outlined as training sets for irrigated hay meadows that are located north and west of the Hayden Powerplant (fig. 1) are illustrated on figure 7.

Using the Image-100 System, the analyst must decide whether or not a spectral signature from a training set is a valid representation of the land-use category of interest. The training set should include only the area occupied by the desired land-cover type. This is complicated when individual pixels contain parts of adjacent land-use types. Attempting to broaden the spectral signature of one class to include the boundary pixels generally produces overlap, so that some pixels are classified as two or more land-cover types (p. 46). If an effort is made to avoid overlap, some pixels remain unclassified. A classification of 85 to 99 percent of the pixels generally is considered adequate for analysis.

A decision was made as to the approximate number of spectrally different land-use classes in the selected part of the image. The results were tested on other parts of the image by applying and evaluating the preliminary spectral signatures (see Glossary). The objective was to check the results that would be obtained in other areas having a different mix of land use.

Analysis of land-use types on the August 24, 1975, image was not completely successful using the Image-100 System. This was because the parallelepiped technique was not always able to differentiate the complex variety of land-use classes with a wide range of lighting conditions (direct sunlight to almost complete shade) in the mountainous terrain characterizing the region. For example, it was determined that several classes of range and dryland agriculture had distinctive spectral signatures, but that riparian vegetation along the streams did not have enough areal extent or density to produce a good training area or a unique signature. Also, the recently worked areas of surface mines proved to have the same signature as other areas of bare soil and rock (that is, sparse vegetative cover), and recently reclaimed surface-mine areas had the same spectral signature as some other areas of agricultural land. In general, most boundary areas between different land-use categories either were classified as more than one category or were left unclassified.

To demonstrate land-cover classification, broad categories of land use were obtained by combining signatures on this Landsat image. The following

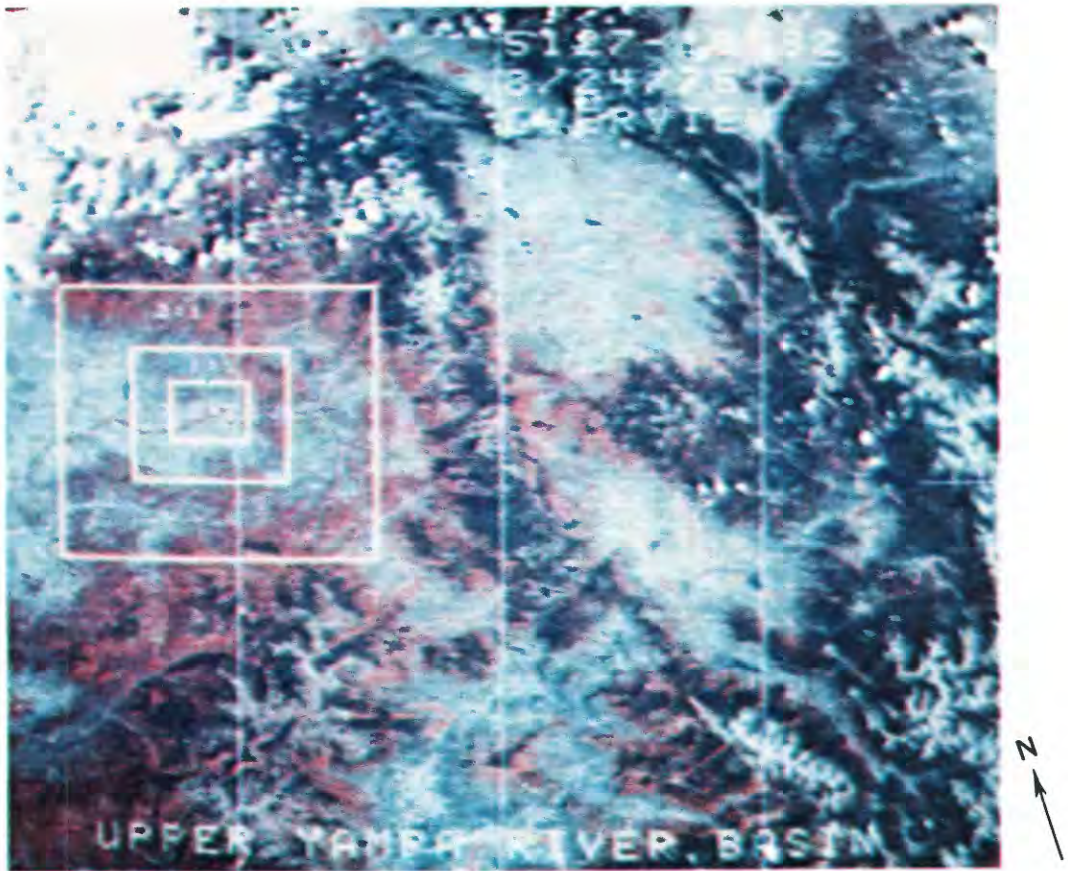


Figure 6.--Selected parts of the August 24, 1975, Landsat image chosen for detailed study.



Figure 7.--Enlarged part of August 24, 1975, Landsat image (fig. 6) with training sets for irrigated hay-meadow class outlined.

class areas (fig. 8) were determined for that part of the image adjacent to the Hayden Powerplant (fig. 1):

<i>Class</i>	<i>Color code</i>
Deciduous vegetation-----	Light blue.
Wet/irrigated hay meadow-----	Red.
Rangeland-----	Purple.
Dryland agriculture-----	Yellow/tan.
Water-----	Dark blue.

About 10 percent of the pixels remained unclassified, and accuracy of the class areas was not evaluated, because of lack of ground-survey information obtained during the same time as the imagery.

Despite the problems with classification of complex land-use signatures, the Image-100 System proved useful to resolve many of the problems confronted in analyzing the August 24, 1975, image. The rapid operation of hardwired functions proved ideal for initial selection and evaluation of spectral signatures of different levels of land-use categories. This exercise provided information on the land-use categories and the level of detail for each category that could be defined using digital analysis.

A map showing major landmarks (roads and rivers) also was registered to the Landsat image through a trial-and-error procedure to evaluate overlay capabilities. A mask of the drainage-basin boundaries then was digitized. Many landmarks were visible on the August 24, 1975, Landsat image, and it proved easy to register a map to the image. This process requires approximately 30 minutes using the Image-100 System.

Land use on the August 24, 1975, Landsat scene also was mapped using the IDIMS. The emphasis was on determining the types and detail of land uses that could be identified with some confidence from the imagery. Two classification techniques were applied to the digital data using this system--unsupervised or clustering techniques (p. 46) and supervised classification with a maximum-likelihood classifier (p. 46).

Primary emphasis was placed on the supervised-classification approach using the IDIMS because of the spectral variability present within a given land-use class. Clustering was applied only to a small part of the imagery to evaluate the correlation between the classes selected by this technique and the actual land-use or land-cover classes as interpreted from 1:24,000-scale black-and-white aerial photographs.

A region displayed on figure 9, encompassing an area extending from the Williams Fork Mountains on the south to the Elkhead Mountains on the north and from Cedar Mountain on the west to the town, Hayden, Colo., on the east



Figure 8.--Image-100 land-use classification of the Hayden Powerplant area.
Refer to text for the color-code identification.

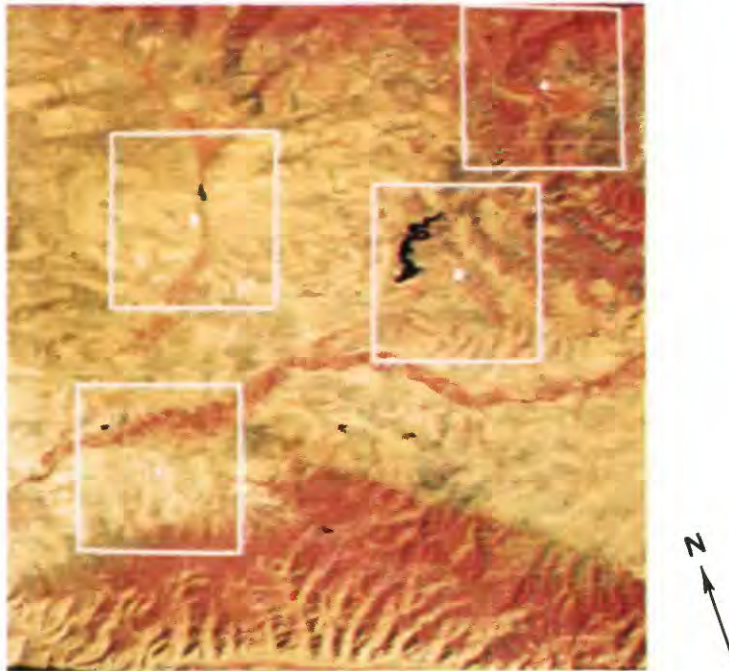


Figure 9.--Enlarged part of the August 24, 1975, Landsat image with four areas outlined.

(fig. 1), was selected for initial development of training sets for various land-use classes. Four areas on figure 9 were chosen for possible use in selecting training sets. These four areas were selected because they contained the majority of land-use and vegetative-cover types present in the eastern one-half of the Yampa River basin.

Unsupervised classification was applied to area 1. The system was instructed to divide all of the pixels within area 1 into 20 spectral classes. Although the spectral separation for all of the 20 classes was good, the resulting spectral classes did not correlate well with land-use or vegetative-cover classes. For example, a specific land-use class would include several spectral classes. Water was the single exception, because its spectral characteristics were unique. Limited correlation between spectral classes selected by clustering and actual land-use classes undoubtedly is caused by a combination of the spectral variability within a particular land-use class and division of the area into too many spectral classes (20 groups). Both of these factors could result in more than one spectral class within a particular land-use class. Clustering may have given better results if fewer spectral classes had been selected, but time limitations precluded further investigation of this approach.

Several training sets were selected from the four areas for each land-use or vegetative-cover class that could be identified on the imagery. In addition, because clouds and cloud shadows were present in other parts of the imagery, training sets were selected for these features as well. This was done because the maximum-likelihood classifier used by IDIMS segregates all pixels in the image into one of the preselected land-use classes. Most of the training-set selection was done within the four areas delineated on figure 9. However, training sets for conifers, clouds, and cloud shadows were selected from other, more appropriate areas on the imagery. Maximum detail within each of the four areas was obtained by expanding each of the areas to fill the display monitor. This allowed individual pixels to be identified. Training sets for each land-use class were located on the imagery primarily by reference to the appropriate black-and-white aerial photographs, topographic maps, and field-reconnaissance data.

Several training sets outlined by polygons in area 2 are illustrated on figure 10. Any number of training sets may be selected for each land-use class that is identified. When the selection of training sets is completed, the computer records the distribution of spectral values for each land-use class and calculates the necessary statistics to define the spectral signature of that land-use class.

A series of two-dimensional plots of the distribution of pixel values for land-use classes can be used to evaluate the spectral separation between classes. These plots consist of ellipses that show the distribution of data between two spectral bands for each of the selected land-use classes. The area inside an ellipse represents the data (plotted in two-dimensional space) that are within one standard deviation from the mean for that class.



Figure 10.--Enlargement of area 2 (fig. 9) with training sets for water and rangeland classes outlined.

Initial land-use and land-cover classes that were selected are listed in table 3. A two-dimensional plot between Landsat bands 5 and 7, which illustrates the ellipses for all land-use and land-cover classes, is shown on figure 11. All combinations of the four Landsat bands were evaluated. Based on the amount of overlap of spectral signatures between the urban classes and the dryland agriculture and rangeland classes (fig. 11), it was decided to delete the two urban classes. As discussed earlier, urban centers in the basin are relatively small; downtown areas contain gravel and dirt lots, and residential areas generally include a large proportion of grass and trees. These factors make the urban areas spectrally similar to other classes on the summer imagery.

Table 3.--Initial land-use and land-cover classes selected for classification using the Interactive Digital Image Manipulation System

Class number	Class
1-----	Urban.
2-----	Dryland agriculture 1.
3-----	Dryland agriculture 2.
4-----	Urban residential.
5-----	Dryland agriculture 3.
6-----	Rangeland 1.
7-----	Rangeland 2.
8-----	Cottonwood.
9-----	Wet meadow.
10-----	Water.
11-----	Rangeland (sparsely vegetated).
12-----	Bare soil.
13-----	Deciduous vegetation.
14-----	Mixed grass and brush (wet areas).
15-----	Meadow.

The 16 classes selected for the final land-use and land-cover classification are listed in table 4. A two-dimensional plot between Landsat bands 5 and 7, which shows the ellipses for the final land-use and land-cover classes, is shown on figure 12. Several classes show some overlap of spectral signatures; for example, the signatures of cloud shadows (class 16) and water (class 8) (fig. 12). Considerable overlap also is apparent for the signatures for cottonwood (class 6) and other deciduous trees (class 11). Cottonwoods are deciduous trees; however, they are in a class of riparian vegetation which would be desirable to separate as a unique class. Lesser degrees of overlap occur for rangeland (brush and shrub) and cottonwoods, mixed grass and brush (wet areas) and cottonwoods, and rangeland (sparsely vegetated) and dryland agriculture 2. The overlap of signatures between cloud shadows and water posed no major obstacle to the analysis because few clouds were present in the image, but these could be a factor in images containing a large

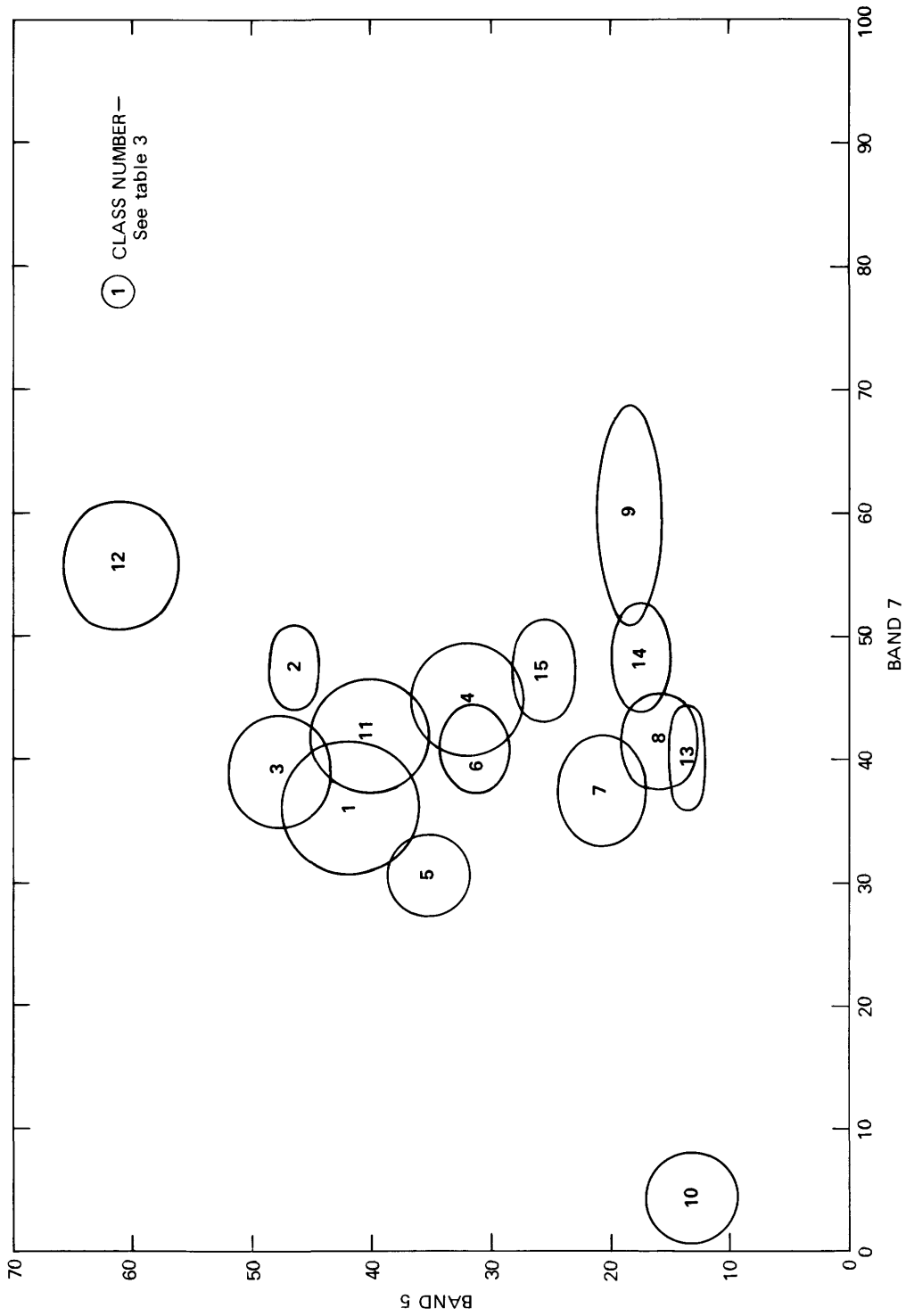


Figure 11.--Two-dimensional plot of spectral distribution within and between initial land-use and land-cover classes using Landsat bands 5 and 7.

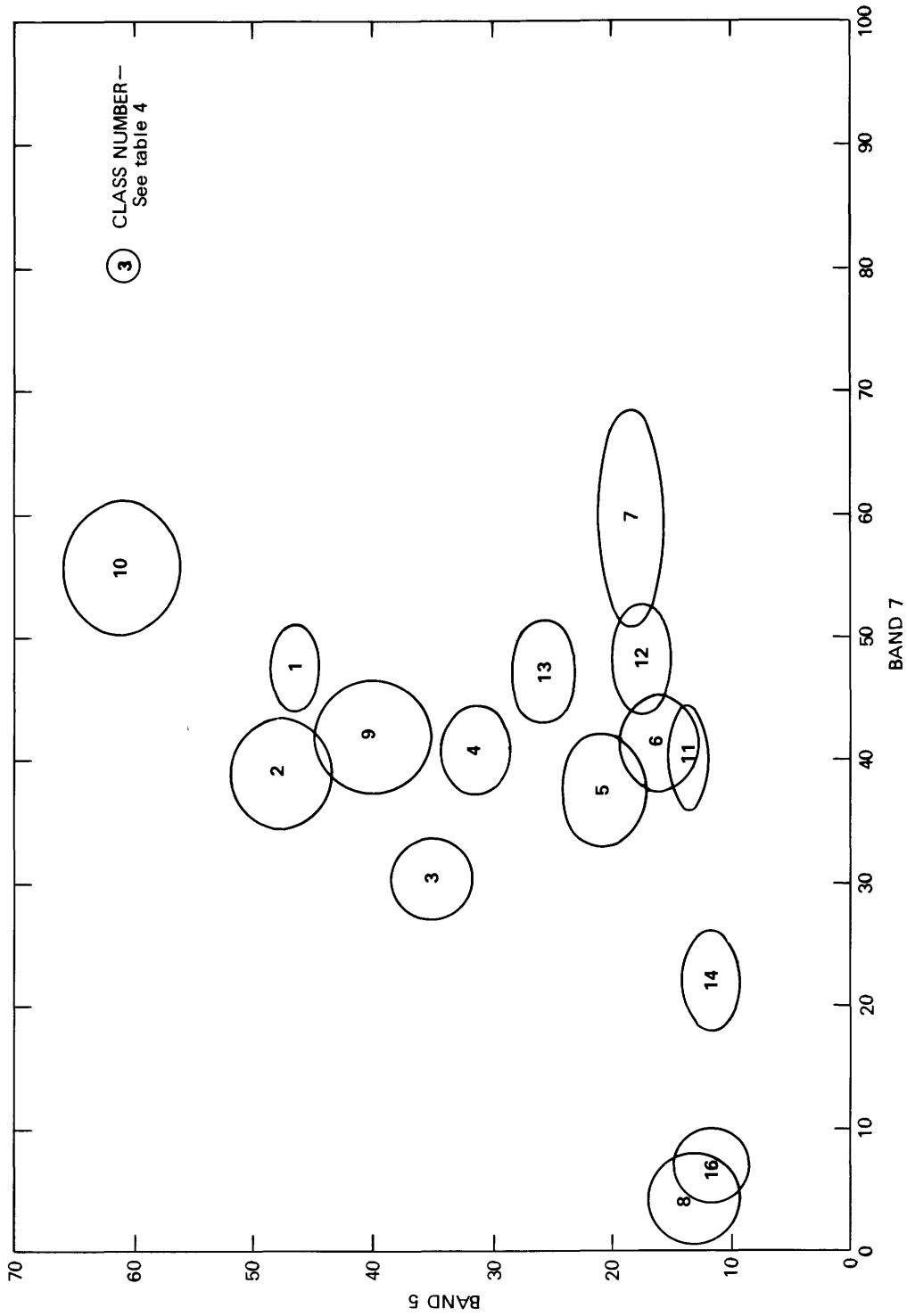


Figure 12.--Two-dimensional plot of spectral distribution within and between final land-use and land-cover classes using Landsat bands 5 and 7. (Class 15, clouds, response was larger than the scale for both bands 5 and 7 and is not plotted.)

Table 4.--*Final land-use and land-cover classes selected for classification using Interactive Digital Image Manipulation System*

Class number	Class	Color code
1-----	Dryland agriculture 1-----	Light green.
2-----	Dryland agriculture 2-----	Olive.
3-----	Dryland agriculture 3-----	Dark green.
4-----	Rangeland (sage and grass)-----	Brown.
5-----	Rangeland (brush and shrub)-----	Orange.
6-----	Cottonwoods-----	Red.
7-----	Wet meadow-----	Aqua.
8-----	Water-----	Dark blue.
9-----	Rangeland (sparsely vegetated)-----	Sand.
10-----	Bare soil-----	Gray.
11-----	Deciduous vegetation-----	Red.
12-----	Mixed grass and brush (wet areas)-----	Aqua.
13-----	Meadow-----	Aqua.
14-----	Conifers-----	Purple.
15-----	Clouds-----	White.
16-----	Cloud shadows-----	Black.

proportion of cloud cover. Overlap of signatures between deciduous trees and cottonwoods precluded the effective separation of these two classes. Although cottonwoods and other deciduous trees were kept as spectrally separate classes, they were displayed on the color-coded classification with the same color. Overlap in signatures between the other classes was minor and probably was caused either by spectral similarity of classes or inaccurate delineation of training sets. The same color-classification code was assigned to wet-meadow (class 7), mixed grass and brush (wet areas) (class 12), and meadow (class 13) classes (table 4) because of physical similarity of classes and a lack of availability of different colors for display purposes.

A color-coded classification of the area along the Yampa River, from the confluence of Elkhead Creek east to about Steamboat Springs, Colo. (fig. 1), is shown on figure 13.

The IDIMS, like the Image-100 System, has the capability of computing total acreages for each of the land-use and land-cover classes selected; however, it was not done for this study because of time limitations and lack of ground information for comparison and confirmation of results. Comparison of land-use classes defined from 1973 black-and-white photographs with ground information and Landsat classification results indicated an increase in dryland-agriculture activity between 1973 and 1975.

Color-infrared aerial photographs of the southern part of the basin were obtained from the U.S. Fish and Wildlife Service (Dennis Parker, written commun., 1977) subsequent to the classification of the Landsat imagery. The



Figure 13.-- Part of a Landsat image showing land-use classification of the region along the Yampa River from confluence of Elkhead Creek to just west of Steamboat Springs. Refer to table 4 for color-code identification.

photography was acquired in July 1976, and provided a more up-to-date reference for evaluation of classification results than the 1973 black-and-white photographs.

Visual comparison of the Landsat classification with the color-infrared aerial photography indicated the following results. Level I land-use delineation generally appeared to be accomplished with very little misclassification, with the following exceptions. One involved urban areas (p. 22). Other possible areas of misclassification occur at boundaries between two or more classes; also, in certain areas in the basin, there appeared to be limited misclassification between agriculture and rangeland classes. This most likely includes either fallow or stubble fields and adjacent areas of sparsely vegetated rangeland. It also was observed that recently reclaimed surface-mine areas (surface-mine areas were not selected as a class because of their small size) were classified as dryland agriculture. These areas have been smoothed over and seeded in grasses, thus appearing similar to agricultural fields on the images. High-wall areas of active surface-mine operations were classified as cloud shadows (black) because of the shadowed areas present. Older unreclaimed mine-spoil areas, were classified as rangeland or sparsely vegetated rangeland.

Results also indicate that in many areas a reasonable level II classification can be obtained for agricultural-land, rangeland, forest-land, water, and wetland classes (table 2). Exceptions, in addition to those discussed for level I classification, include some mixed categories and some classes with small areal extent. Because of lack of detailed ground information, it was not possible to identify specific crop types for the three dryland-agriculture classes (table 4). Areas classified as dryland agriculture and confirmed using the July 1976 aerial photography also indicated a considerable increase in areal extent of dryland-agriculture activity along the Yampa River valley during the last several years, especially between Craig and Milner, Colo. (fig. 1). This was determined by comparison of dryland-agriculture fields appearing on the 1973 black-and-white aerial photographs with those appearing on the 1976 color-infrared images. The greater part of the increased area for dryland agriculture resulted from conversion of rangeland to cultivated fields. Results in level II classification of forest areas appeared to be quite accurate with the exception of zones where oak brush and aspen trees tend to intermix, causing an overlap of rangeland and forest-land classes. Also, irrigated hay meadows, which would technically be included in an agricultural class, virtually were spectrally the same as natural-grass areas along stream drainages, which are in the class of wetlands. Water bodies greater than 5 acres (2 ha) in size were classified accurately in almost all areas, with the exception of some lakes in steep-sided mountain valleys which were obscured by shadows.

In summary, it appears that the Landsat system is a potentially valuable tool for regional land-use classification and update in the Yampa River basin, subject to the exceptions that have been noted previously. Land-use maps for much of the Yampa River basin are already in existence, but these maps already are outdated because of the rapid changes in land use that are

occurring in certain areas of the basin. Results from this preliminary investigation indicate that Landsat data could be used as a screening tool for identification and monitoring of changes in land-use patterns. This is especially true for monitoring conversion of rangeland to dryland agricultural fields. Also, larger strip mines can be monitored for extent of their operation with reasonable accuracy. Other temporal changes in land-use patterns in the Yampa River basin that should be feasible to locate and map using Landsat are: Timber-cutting operations, changes in rangeland condition (large area) as a result of grazing and other factors, and areal extent and location of surface-water storage larger than 5 acres (2 ha). It should be emphasized that, because of the MSS resolution of approximately 1.1 acres (0.45 ha) and other factors discussed concerning the current Landsat system, it is generally not suitable for land-use and land-cover classifications more detailed than level II. It does, however, provide a potentially valuable method for locating areas of change in land-use at level I and in some instances level II. This capability would save a great deal of time and effort in monitoring land-use patterns in a large area, such as the Yampa River basin. Areas requiring more detailed analysis (aerial photography or ground reconnaissance) could be identified by using Landsat images.

The conclusions presented above are based on the qualitative results obtained in the investigation coupled with results obtained by other investigators who have conducted similar studies. In order to quantitatively define the capabilities of this approach in the Yampa River basin, further study is required.

Lineament Mapping

Increasing demand and competition for surface-water resources in the Yampa River basin are resulting in expanded development of ground-water resources. The development of ground-water supplies in this region is just beginning but should increase rapidly in response to pressures for additional water supplies.

Many studies in consolidated-rock terrain have concluded that larger yields may be obtained from wells drilled along or at the intersection of faults or major joints. Landsat imagery provides the large areal coverage necessary to detect major lineaments that may indicate faults or fracture zones with potential for increased ground-water availability (Goetz and others, 1975; Moore and Deutsch, 1975). Lineaments are not always indicative of fractures in the rock, and further investigation usually is required to confirm the presence of a fault or fracture for subsequent ground-water investigation. Even if the results of lineament mapping were only partly successful in locating areas of near-surface ground-water occurrence, the time and funds spent on this procedure could potentially result in considerable reduction in the cost and effort expended in drilling productive water wells.

The band-7 black-and-white winter image for February 26, 1975 (fig. 14), was selected for interpretation of lineaments. This image was chosen because



Figure 14.-- Part of black-and-white image, band 7, of Landsat scene 1948-17084, February 26, 1975.

the low sun angle and subsequent shadows at this time of year enhance topographic features. This image also depicts a thin cover of snow. A thin cover of snow can enhance subtle surface features as a result of contrast between snow and shadows. The reverse also can be true, however. Snow may obscure some of the less pronounced topographic features in certain areas. The results of the interpretation procedure are presented on figure 15. Mapped lineaments are superimposed on the Landsat image for February 26, 1975, and faults depicted on available geologic maps have been superimposed on part of the same Landsat image (fig. 15). Only a small percentage of the mapped faults correspond to the lineaments interpreted in this exercise. This is not necessarily indicative of unsatisfactory results, however, because lineaments can be a manifestation of fractures and faults in the form of both subtle topographic and vegetative trends which were not readily discernible during ground-mapping exercises.

The small scale of satellite imagery allows identification of extended linear trends but may not be suitable for identification of fault zones that do not have extended surface trends. Conversely, subtle linear trends definable on Landsat images may not be visible to geologists conducting surficial mapping. At the present time, sufficient ground-water data are not available in the Yampa River basin for evaluation of the theory that larger yields can be obtained from wells placed along fracture and fault zones. However, many new wells are being drilled in the region which should provide the information necessary for a preliminary evaluation of the correlations between ground-water occurrence and faults or fractures in the near future.

In conclusion, lineaments were mapped from Landsat imagery using general principles of photographic interpretation. However, ground investigation in the Yampa River basin is required to determine if mapped lineaments are indicative of ground-water occurrence in this area. This method may provide a rapid means of initial ground-water exploration for this and similar regions if the correlations, obtained by other investigations, between faults and fractures and larger yields of ground water hold true.

Mapping Areal Snow-Cover Extent

The melting of mountain snowpack in the spring is the source of greater than 50 percent of the annual streamflow in most areas of the western United States (Committee on Polar Research, 1970; Rooney, 1969). Approximately two-thirds of the total annual streamflow of the Yampa River is supplied by the snowmelt runoff (Steele and others, 1978). Estimation of water equivalent of snow is required for accurate forecasting of water availability derived from the snowpack. This forecasting requires periodic timely information on snowpack condition and extent. The most common forecast method currently uses water-equivalent values obtained at selected points to infer conditions for the remainder of the watershed. Point data may not be representative of conditions for the entire watershed. Recently, investigators have found positive relationships between areal extent of the snowpack and subsequent runoff amounts (Leaf, 1971; Brown and Hannaford, 1975).

EXPLANATION
 — FAULT
 — LINEAMENT



Figure 15.-- Lineament and fault map superimposed on Landsat scene 1948--17084, February 26, 1975.

Landsat data can provide the information necessary to map areal snow extent in large watersheds (Barnes and Bowley, 1974). This information, used in conjunction with traditional ground surveys, may increase the accuracy of forecasting runoff amounts. The increased accuracy of forecast would improve the efficiency of allocating water derived from seasonal snowpack.

The Image-100 System was selected for determination of areal snow extent. Digital tapes of the February 26, 1975, Landsat image (fig. 14) were used for this analysis. The Image-100 System was selected for use in this application because it provided the opportunity to map only those areas within the Yampa River basin boundaries and because spectral complexity was not a significant factor in this image, so the faster parallelepiped-decision function was suitable for classification.

In cloud-free areas of the western part of the Yampa River basin, deep snow in open areas has a distinctive spectral signature, with large digital values in all four Landsat bands. It was a simple matter to define a training set for any small area and to subsequently classify all open areas covered by deeper snow.

The Landsat image included many areas with digital values less than those for deeper snow in open areas but much greater than those for other land-cover types. These areas were classified qualitatively as thin or partly shadowed snow, and very thin or shadowed snow. Shadowed snow is most likely the result of various densities of exposed vegetative cover. Ground surveys would be needed to determine whether the snow in these areas was deep enough to be significant for predicting future streamflows. In relatively open areas of thin snow, Landsat data might be used to show the areal extent of snow thickness, as measured at a few points on the ground. In open areas of thicker snow, however, present Landsat data provide no information on thickness, water equivalent, or free-water content.

Clouds have approximately the same spectral signature as snow, and cloud shadows obscure land-cover features. Some cloud cover is common in the Yampa River basin during the winter and could cause problems in delineating snow extent on some of the Landsat images.

Concern has been expressed by some scientists about snow areas being obscured by dense conifer forests (Rango, 1975, p. 61, 231). This did not appear to be a major problem in the snow-covered areas of the western part of the Yampa River basin. In this area, there are few stands of dense conifers, and many groups of conifers occupy less area than the 1.1 acres (0.45 ha) of a Landsat pixel. Thus, most of the deep-snow class appeared to be continuous on this Landsat image. However, in mountainous areas of the eastern part of the basin, which supply the majority of the snowmelt runoff, conifer stands are dense in many locations and could create problems in digital classification.

A basin-boundary map was registered and digitized similarly to the approach discussed previously for the August 24, 1975, Landsat-image land-use analysis. However, in this instance, map registration was a time-consuming

process, because few landmarks were visible on the Landsat image in areas of snow cover. With the basin-boundary data, the areas of snow cover within the western part of the Yampa River basin included in the Landsat image (fig. 2) could be determined (fig. 16). The computer sums the pixels in each class and calculates the area included in each class. The following arbitrary snow-depth categories were determined for the western part of the basin (fig. 16):

<i>Category</i>	<i>Color code</i>
Thick snow-----	Red.
Thin snow or partly shadowed snow----	Yellow.
Very thin or shadowed snow-----	Blue.

In summary, results from this preliminary investigation indicate that Landsat imagery in some instances can provide timely information on areal snow extent over large regions. Snow in open areas generally is easily defined; however, snow under densely forested areas may be difficult to map using Landsat imagery alone. Also, cloud cover can cause problems in misclassification when using digital-analysis techniques or when it obscures surface areas preventing effective classification of those segments on the image when using photographic-interpretation techniques.

Although digital analysis was investigated in this study, other studies (Barnes and Bowley, 1974) indicate that, for many areas, mapping of snow-area perimeters by manual (photographic-interpretation) means may provide the desired information on areal snow extent while allowing subjective decisions on cloud-obscured areas and snow contained under dense conifer stands. The photographic-interpretation method generally would be available to more agencies, because less sophisticated equipment is required. Also, photographs of Landsat images can be obtained more rapidly subsequent to acquisition than the computer-compatible digital tapes required for digital analysis.

Turbidity Estimation

Expansion of surface-mining, construction, and dryland-agricultural activities is increasing the potential for greater turbidity and sediment levels in the basin's streams. Aerial photography used in conjunction with a few ground-control data points may prove to be a rapid alternative to time-consuming extensive ground surveys required for assessing turbidity in streams over large areas of the basin (Ritchie and others, 1976). Photographic coverage of streams encompassing a large area could be obtained in a very short time period relative to the time required for ground sampling of the same areas with limited manpower. In theory, changes in turbidity in a water body should cause changes in reflected energy recorded on photographs. This change in reflectance is clearly visible on photographs for extreme variations in turbidity. This investigation was designed to

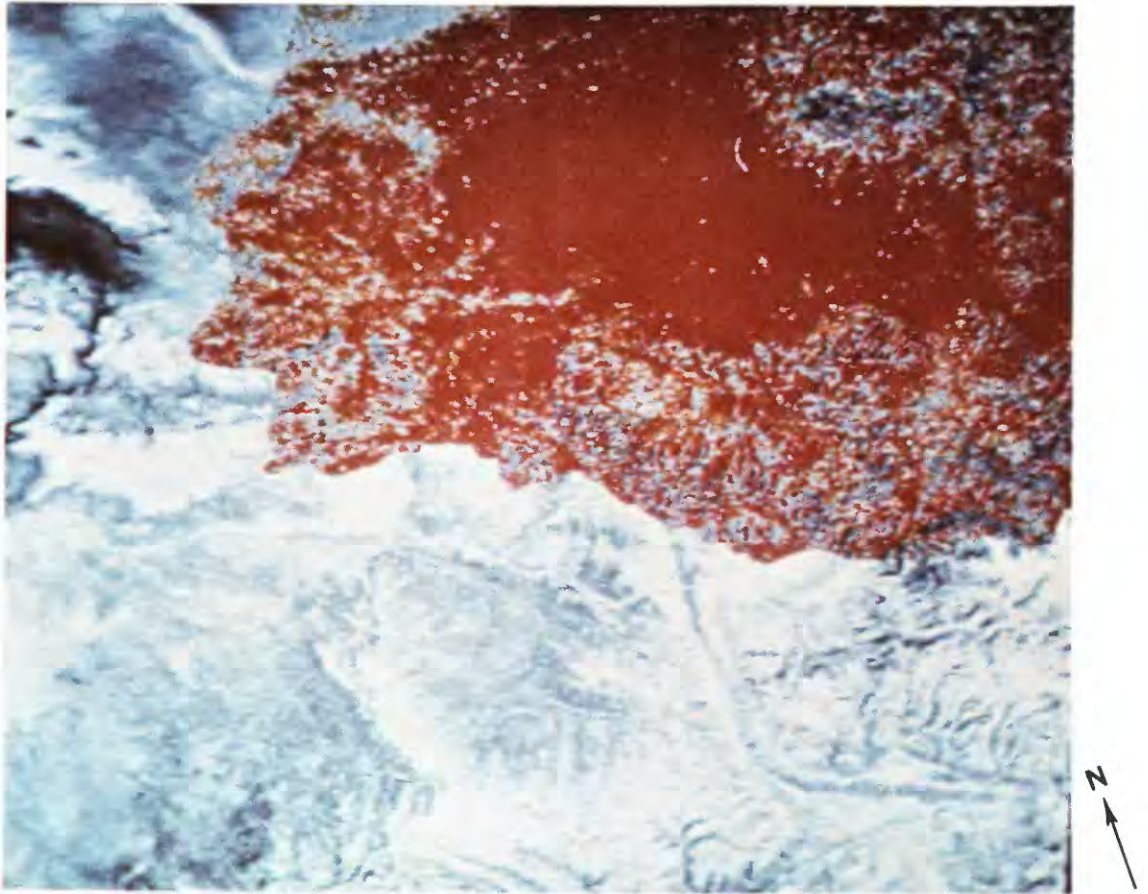


Figure 16.--Snow--cover classification of Yampa River basin part of the February 26, 1975, Landsat image. Refer to text for color--code identification.

evaluate the sensitivity of color and color-infrared photographs to changes in turbidity and further to determine if turbidity could be indirectly measured (quantitatively) using the photographs. If a correlation between reflectance and turbidity does exist, then only a few selected ground-sampling points should be required to calibrate the reflectance levels appearing on the aerial photographs with measured turbidity values.

This investigation was planned so that the aerial photographs and the ground information would be acquired during the period of peak snowmelt runoff, in order to insure a wide range of turbidity values. Approximately 30 ground-sampling sites initially were selected in mid-May for collection of turbidity and suspended-sediment samples to coincide with the acquisition of aerial photographs.

However, due to scheduling conflicts and limited manpower, turbidity and suspended-sediment samples were collected at only eight stations on three streams at approximately the same time as the overflight during which the color and color-infrared photographs were acquired. Sampling-station locations are depicted on figure 17. Individual sampling stations and the turbidity and suspended-sediment values obtained during the ground sampling are presented in table 5.

Table 5.--*Turbidity and suspended-sediment measurements obtained May 31 and June 1, 1977*

Date	Site ¹	Turbidity, in Formazin turbidity units	Suspended-sediment concentration, in milligrams per liter
<i>1977</i>			
May 31-----	Y-47	4	29
May 31-----	Y-64	4	16
May 31-----	Y-71	3	68
June 1-----	Y-0A	8	34
June 1-----	Y-1	48	402
June 1-----	Y-17	9	51
June 1-----	Y-39	4	42
June 1-----	Y-40	11	23

¹See figure 17.

Positive-color and color-infrared transparencies were used for comparison of spectral reflectance and measured turbidity values. The auxiliary television camera associated with the Image-100 System was employed to digitize the parts of the transparencies depicting the segments of the

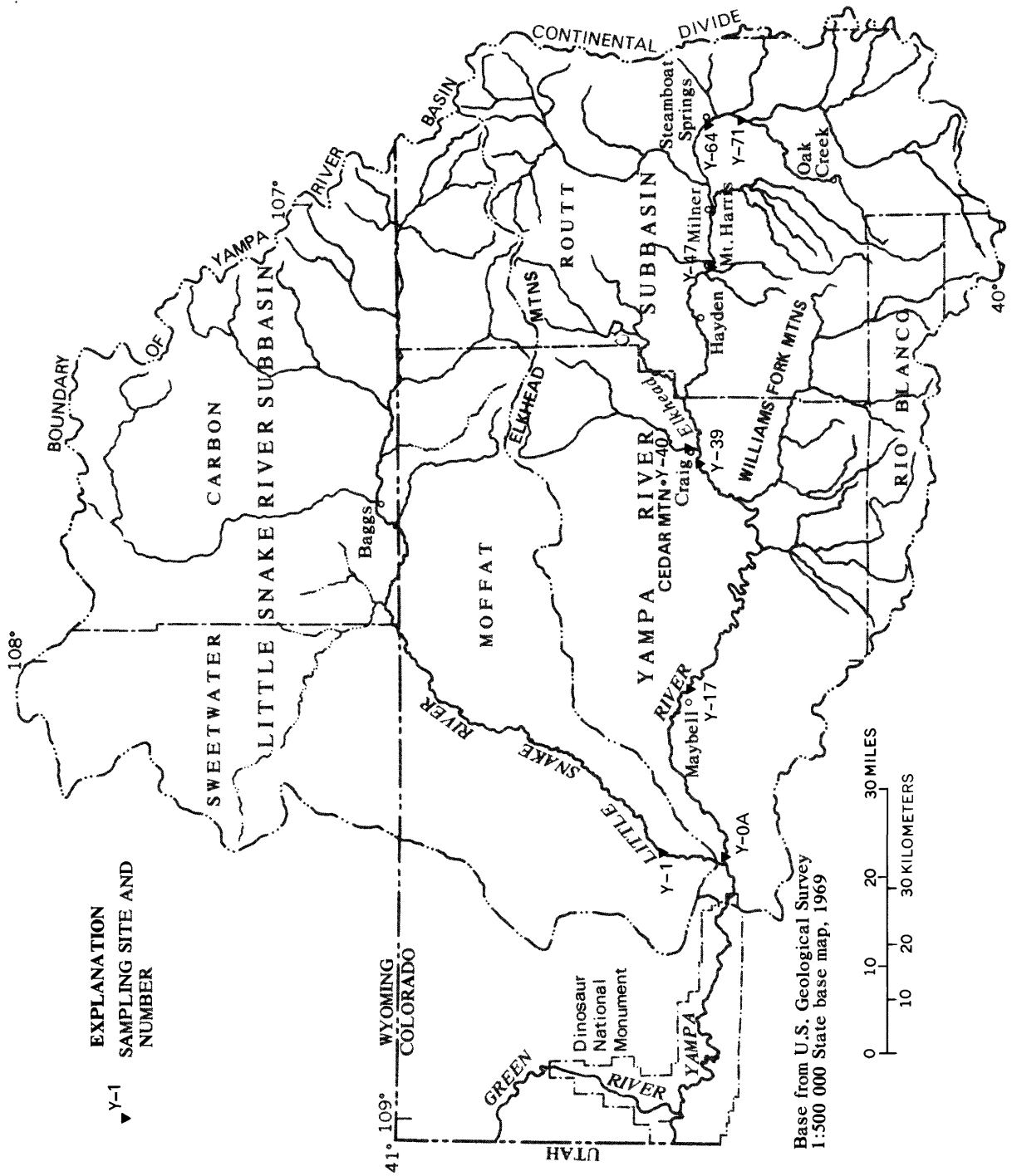


Figure 17.--Locations of sampling sites for the turbidity/spectral-reflectance investigation.

streams for which water samples had been collected and analyzed (fig. 17). The analog data from the television-camera system were converted to digital values for analysis using the Image-100 System.

Both the color and the color-infrared film have three emulsion layers. These layers are sensitive to blue, green, and red wavelengths of light for color film, and green, red, and near-infrared wavelengths of light for color-infrared film. Each of these light-sensitive layers was digitized separately by using the appropriate filters on the television camera to mask out the light from the other two layers. This, in effect, provides three spectral bands of information for each transparency that is digitized.

The Image-100 System was used to generate the range and mean values of the digital numbers (reflectances expressed as digital values) in each of the three spectral bands depicted on the photographic transparencies. This was accomplished for each of the eight sampling stations listed in table 5 using both the color and the color-infrared transparencies. The color-infrared transparencies did not contain sufficient contrast in this instance for correlation with turbidity values, so no further analysis was accomplished using these data.

The digital numbers and their statistics obtained from the color transparencies are presented in table 6. The graphic relationship between measured turbidity values and mean digital values for each of the spectral bands is shown on figure 18. Additionally, a set of second-order polynomial regressions was developed from these data which use mean digital numbers to predict turbidity for each of the spectral bands. Regression equations and associated statistics including R^2 (goodness of fit) values are presented in table 7.

Table 6.--*Digital reflected-energy values and associated statistics calculated from analysis of color transparencies*

Site ¹	Blue layer			Green layer			Red layer		
	Range	Mean	Variance	Range	Mean	Variance	Range	Mean	Variance
Y-0A--	6-14	10.1	3.8	12-23	18.8	9.2	3-12	7.4	3.9
Y-1---	14-20	17.5	6.8	32-47	41.0	31.5	13-18	16.0	4.5
Y-17--	7-13	9.6	1.4	9-15	13.0	2.8	4-11	7.0	2.7
Y-39--	3-8	5.4	1.2	5-12	9.2	3.4	1-8	2.4	1.7
Y-40--	10-10	10.0	0.0	27-27	27.0	0.0	9-9	9.0	0.0
Y-47--	5-9	7.5	1.5	5-13	10.6	4.1	0-9	4.9	2.0
Y-64--	3-7	4.5	2.3	8-14	10.0	5.5	0-2	1.0	0.5
Y-71--	2-6	3.8	3.2	1-5	3.3	2.2	0-3	1.8	1.7

¹See figure 17.

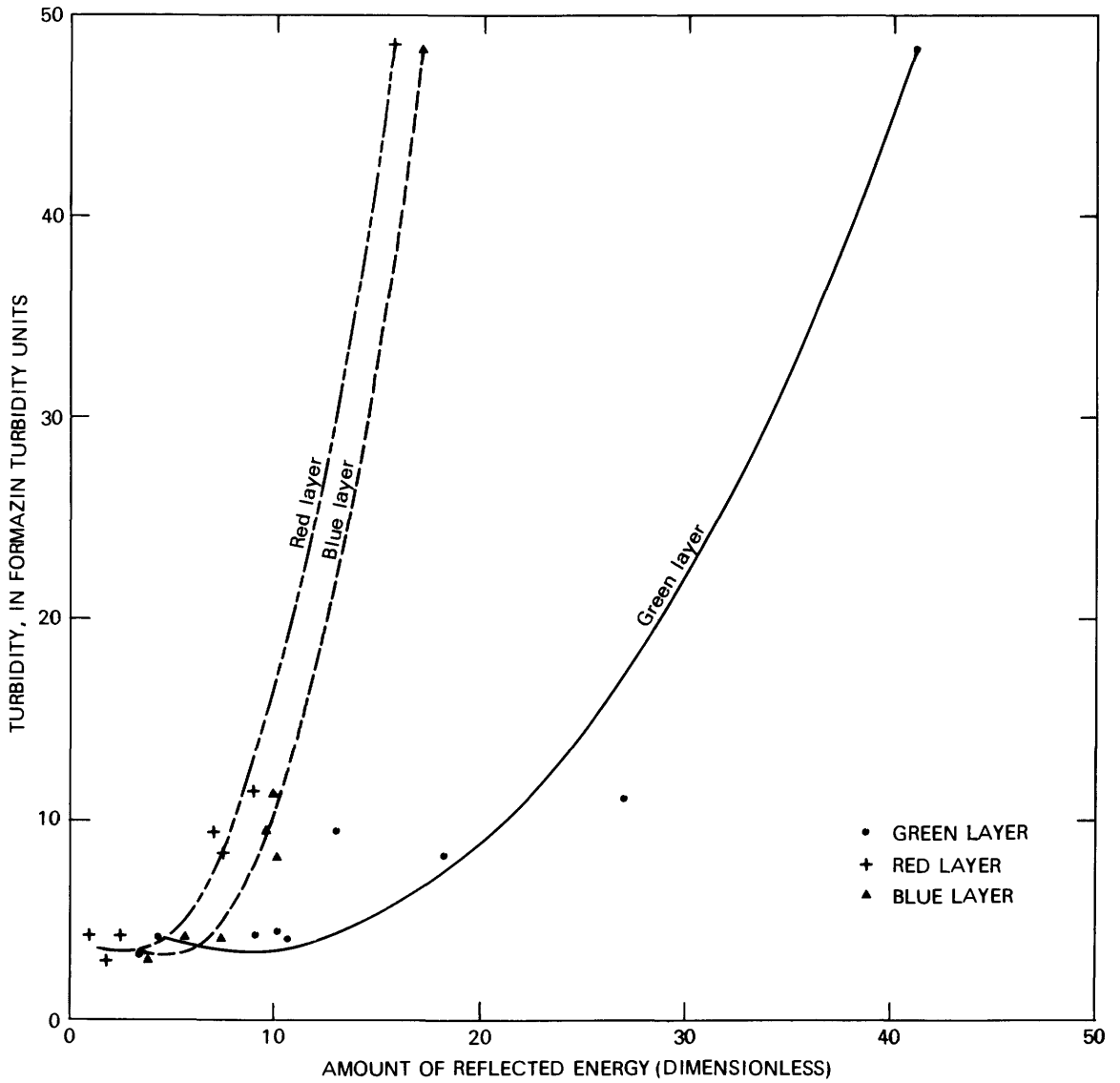


Figure 18.--Mean digital reflected-energy values versus turbidity values for the three spectral bands (layers): Blue, green, and red.

Table 7.--Regression equations and associated statistics developed for prediction of turbidity

[Y=turbidity (Formazin turbidity units); X=digital number; sample sites=8]

Emulsion layer	Regression equation	Goodness of fit (R^2)	Standard error of estimate (s)
Blue----	$Y=12.02-3.30(X)+0.31(X^2)$	0.99	1.16
Green---	$Y= 8.13-0.88(X)+0.04(X^2)$	0.96	3.33
Red-----	$Y= 5.63-1.63(X)+0.27(X^2)$	0.99	1.03

Results of this analysis show a correlation (R^2 greater than 0.90) between mean digital numbers in the spectral bands and measured turbidity values. It appears that the red and blue spectral bands are more suitable for inferring smaller values of turbidity. The green band appears to be more responsive for larger values of turbidity.

Comparison of measured turbidity and suspended-sediment concentrations provided no well-defined correlations between the two variables in this investigation. Results obtained from comparison of spectral reflectance with turbidity indicate that aerial photography potentially could be used to infer turbidity of streams, with minimal ground-data collection. Several factors combined to provide less than ideal conditions for this investigation. The volume of snowmelt runoff for the spring of 1977 was much less than average and occurred during the first 2 weeks in May. Due to conflicts in aircraft scheduling and weather conditions, acquisition of the aerial photographs was delayed until May 31, about 3 weeks after the peak runoff period. In addition, because of deteriorating weather conditions, photographs on this date were obtained only for the southern part of the basin, thus omitting the greater part of the Little Snake River and its tributaries (fig. 3). Therefore, additional studies with more data points and a wider range of turbidities will be required to substantiate the correlations indicated by the results of this study. However, the results of this investigation are encouraging and further study is warranted.

FUTURE CONSIDERATIONS

Based on the experience gained during this study, several modifications and additions to analytical procedures are suggested to improve classification accuracies and allow quantitative evaluation of results. Adequate ground information and aerial photographs (1:24,000 scale, or smaller), acquired during the same general time period (preferably during the same season) as the satellite imagery would be valuable in this respect.

They would aid in the selection of appropriate training sets for supervised classification, determination of the number of classes that are present, and determination of the level of detail for classification. Selection of well-defined representative training sets is essential to the successful application of a supervised classification approach. However, classification of pixels (see Glossary) which include mixtures of classes still present a problem. Additional studies need to be conducted to determine the optimum time of the year for best discrimination of various classes of interest, especially for land-use classification.

No single time of year is ideal for separation of all land-use classes. The detail of classification compared with cost-benefit considerations will indicate if a multitemporal analysis should be used or if a single time period will suffice.

A better understanding of the spectral characteristics of various land-use and land-cover classes might help to improve classification results. This may be most helpful in determining the applicability of cluster-type analysis for certain areas. It is also possible that other image-processing systems may have capabilities which would provide better results in classification. However, most systems currently being used seem to have similar capabilities for general classification of satellite imagery (Carter and others, 1977).

Overlaying (merging) of various types of supplementary data, such as map and photographic information, with satellite imagery may prove to be cost effective in some instances and would allow greater flexibility in classification of both land use and areal snow cover. For example, incorporation of topographic information with the Landsat images might be used as a method to infer snow presence under a forest canopy. This could be done using slope, aspect, and altitude of areas where snow cover is visible to infer snow in similar topographic areas which are densely forested.

Future plans for this study include possible analysis of the color and color-infrared aerial photographs for other geologic, hydrologic, and land-use applications. Further definition of land-use and land-cover classes may be conducted in conjunction with analysis of summer 1977 Landsat images to provide some quantitative measure of classification results.

Continued investigations using aerial photographs to infer areal-turbidity variations in streams are planned. The use of lower altitude photography may improve resolution and allow incorporation of turbidity from smaller tributaries. It appears that a system as simple as a 35- or 70-mm camera vertically mounted on a small aircraft would be suitable as a data-collection system. This would allow extensive coverage of desired stream reaches with a relatively small cost of acquisition and subsequent processing of photographs.

Additional satellites are scheduled to be operational within the next few years. These will provide increased resolution, new wavelength bands for more effective discrimination between surface features, thermal sensors, and

active and passive microwave systems. In addition, more geostationary satellites which provide high-frequency observations of a specific area are planned. The continued advancement in satellite technology should expand considerably the future applications of these systems. In conclusion, the investigations conducted in this study indicate that satellite images and aerial photographs can be cost effective, in many cases, when used in conjunction with other traditional means, for timely regional assessment of the variables discussed.

REFERENCES

- Anderson, J. R., Hardy, E. E., Roach, J. J., and Witmer, R. E., 1976, A land use and land cover classification system for use with remote-sensor data: U.S. Geological Survey Professional Paper 964, 28 p.
- Barnes, J. C., and Bowley, C. J., 1974, Handbook of techniques for satellite snow mapping: Environmental Research and Technology Inc., no. 0407-A, 93 p.
- Brown, A. J., and Hannaford, J. F., 1975, Interpretation of snowcover from satellite imagery for use in water supply forecasts in the Sierra Nevada, *in* Operational applications of satellite snowcover observations: Washington, D.C., National Aeronautics and Space Administration Special Paper 391, p. 39-51.
- Carter, V. P., Billingsley, F. C., and Lamar, Jeannine, 1977, Summary tables for selected digital image processing systems: U.S. Geological Survey Open-File Report 77-414, 45 p.
- Colorado Water Conservation Board and U.S. Department of Agriculture, 1969, Water and related land resources, Yampa River basin, Colorado and Wyoming: Denver, Colo., Colorado Water Conservation Board, 163 p.
- Committee on Polar Research, 1970, Polar research--A survey: Washington, D.C., National Research Council, National Academy of Sciences, 204 p.
- Goetz, A. F. H., Billingsley, F. C., Gillespie, A. R., Abrams, M. J., Squires, R. L., Shoemaker, E. M., Lucchitta, I., and Elston, D. P., 1975, Application of ERTS images and image processing required in geologic probing and geologic mapping in northern Arizona: Pasadena, Calif., Jet Propulsion Laboratory, Technical Report 31-1597, 118 p.
- Leaf, C. F., 1971, Areal snow cover and disposition of snowmelt runoff in central Colorado: Fort Collins, Colo., U.S. Department of Agriculture, Forest Service, Research Paper RM-66, 19 p.
- Moore, G. K., and Deutsch, Morris, 1975, ERTS imagery for ground water investigations: Ground Water, v. 13, no. 12, p. 214-226.
- National Aeronautics and Space Administration, 1977, Landsat data users handbook: Washington, D.C., Document 76SD54258, 67 p. and 13 app.
- Rango, Albert, ed., 1975, Operational applications of satellite snowcover observations: Washington, D.C., National Aeronautics and Space Administration Special Paper 391, 430 p.
- Ritchie, J. C., Schiebe, E. R., and McHenry, J. R., 1976, Remote sensing of suspended sediments in surface waters: Photogrammetric Engineering and Remote Sensing, v. 42, no. 12, p. 1539-1545.

- Rooney, J., 1969, The economic and social implications of snow and ice, *in* Chorley, R. J., ed., *Water, earth and man*: London, Methuen and Company, Ltd., p. 389-401.
- Routt County Soil Conservation District, 1977, Sediment yields resulting from land use activities in Routt County, Colorado: [U.S.] Environmental Protection Agency Section 208 Report, Prepared for Routt County Department of Environmental Health, Steamboat Springs, Colo., June 1977, 11 p. and app.
- Steele, T. D., Bauer, D. P., Wentz, D. A., and Warner, J. W., 1978, The Yampa River basin, Colorado and Wyoming--A preview to expanded coal-resource development and its impacts on regional water resources: U.S. Geological Survey Water-Resources Investigations 78-126 [in press].
- Steele, T. D., James, I. C., II, Bauer, D. P., and others, 1976, An environmental assessment of impacts of coal development on the water resources of the Yampa River basin, Colorado and Wyoming--Phase-II work plan: U.S. Geological Survey Open-File Report 76-368, 33 p.
- Udis, Bernard, and Hess, R. C., 1976, Input-output structure of the economy of Routt and Moffat Counties of the Yampa River basin in Colorado, 1975: Completion report for U.S. Geological Survey Contract P.O. 12166, 146 p.
- Wiedel, J. W., and Kleckner, Richard, 1974, Using remote sensor data for land use mapping and inventory--A user guide: U.S. Geological Survey Inter-agency Report 253, 12 chaps. and app.

SUPPLEMENTAL INFORMATION

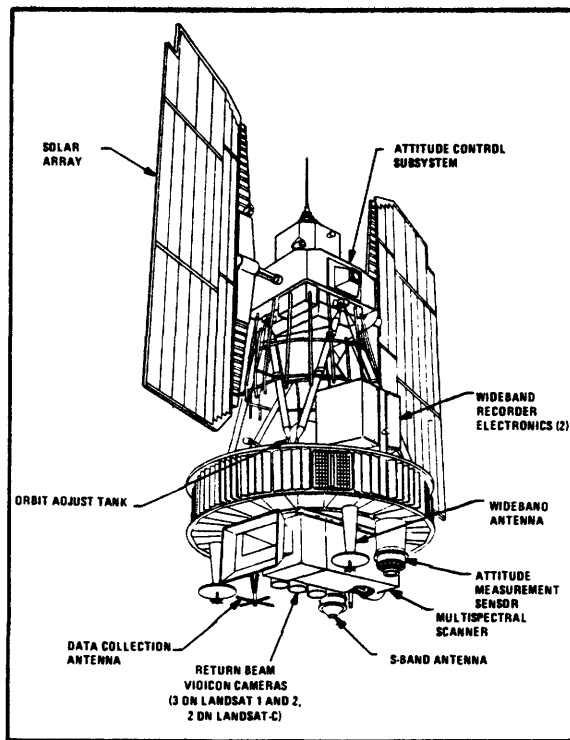
Landsat System

Landsat (fig. 19A) is an experimental National Aeronautics and Space Administration satellite designed to demonstrate the feasibility of mapping and monitoring surface features of the earth from space. The Landsat orbit is near circular, sun synchronous (see Glossary), and nearly polar (81° inclination) with an average altitude of approximately 586 mi (990 km). This orbit provides full earth coverage by a satellite, except for the polar regions, every 18 days. No observations are made within a cone of about 18° around the poles because the orbit of the satellite is not exactly polar. The orbit paths are maintained so that image centers of repetitive views vary no more than 19 mi (30 km) along the orbit path and 23 mi (37 km) perpendicular (right angles) to it. The area of the earth's surface covered by each Landsat image is approximately 115 by 115 mi (185 by 185 km), or about 13,000 mi^2 (34,000 km^2).

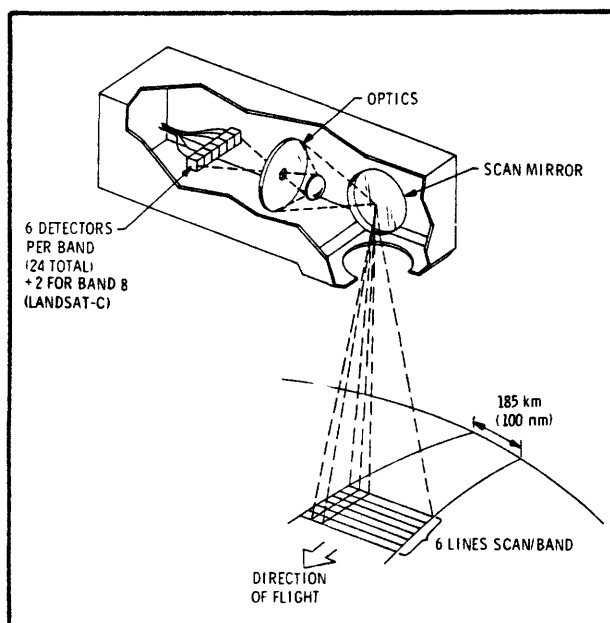
Landsat carries an instrument package composed of three return-beam Vidicon (RBV) cameras, a multispectral scanner system (MSS) (fig. 19B), data-collection relays, and video-tape recorders. Data from the RBV were not used in this study so no further discussion of this system will be presented here. The spatial resolution of each pixel (see Glossary) acquired by the MSS is approximately 1.1 acres (0.45 ha) at the earth's surface which results in about 7.6 million pixels per image.

The MSS system consists of four sets of electro-optical sensors, each containing six detectors. Each set is filtered to record light from a separate part of the electromagnetic spectrum, thus producing four reflected-energy values for each pixel. The spectral bands of the four MSS sensors are: Band 4, green (0.5 to 0.6 μm); band 5, red (0.6-0.7 μm); band 6, near infrared (0.7-0.8 μm); and band 7, near infrared (0.8-1.1 μm).

Imaging is accomplished by collecting light from the earth's surface via the scanner system and passing it through a telescopic system to four filtered sets of optical fibers (fig. 19B). The light is routed to a series of photomultiplier tubes, providing electrical energy, which is subsequently converted to digital values and then telemetered to receiving stations on the ground. The digital values correspond to the amount of reflected energy received by the sensors. Data are stored in digital format and can be used to produce black-and-white, single-band, and color-composite photographs, and computer-compatible tapes. Further information on the Landsat system can be obtained from the Landsat Data Users Handbook (National Aeronautics and Space Administration, 1977).



A. Landsat configuration



B. Multispectral scanner system (MSS) scanning arrangement

Figure 19.--Sketches showing *A*, Landsat configuration; and *B*, Multispectral scanner system (MSS) scanning arrangement. (Adapted from National Aeronautics and Space Administration, 1977.)

Photographic-Interpretation and Digital-Analysis Techniques and Equipment

Photographic Interpretation

Photographic interpretation, generally defined for this study, is the identification of surficial features from photographs and the determination of their meaning or significance. Surficial features are identified from photographs by characteristic clues, such as shape, size, tone, pattern, shadow, and texture. The combination of the human eye and the brain allow the integration of the above clues for interpretation of features. Both subjective judgments and deductive reasoning are used by the experienced photointerpreter in the interpretation process. The primary advantage of photographic interpretation techniques is that they do not require the use of computer systems to complete an analysis. The equipment required can be as little as a photograph and an individual with experience in interpretation techniques. Therefore, materials required for this approach are generally considerably less costly than those required for digital analysis of images.

Digital-Analysis Techniques

Digital-data processing, as applied in this study, refers to computer processing and classification of digitally formatted images. Advantages and disadvantages of using this approach are listed below:

Advantages:

1. When the images are in digital form, large volumes of data can be processed and classified more easily and rapidly than can be classified by photographic-interpretation techniques.
2. A digital format is easily adaptable to transformations which may enhance the original image for specific applications.
3. A digital format readily allows overlay and registration of diverse data types--for example, maps superimposed on images or overlay of images from the same location but for different dates.
4. Digital analysis facilitates the establishment and location of sampling units and the statistical analysis of both original and classified data. It also allows rapid computation and display of areal extent of data classes.
5. Digital data can be produced in a variety of formats and scales.

Disadvantages:

1. Computer-compatible digital tapes of images generally are more expensive than photographic renditions.

2. Analysis requires access to a computer hardware/software system suitable for digital processing.

3. Digital-image processing generally cannot compare to the human eye and brain combination for integration of spectral and spatial characteristics contained in an image. Therefore, classification of data by most digital-image-processing systems uses only spectral information. This disadvantage is lessened somewhat when an interactive image-processing system with a color-display monitor is used so that photographic-interpretation techniques can be incorporated with digital processing.

Two basic types of classification functions were used in digital analysis of data for this study--supervised and unsupervised. The supervised classification technique has two options--use of a maximum-likelihood classifier or the parallelepiped-decision function without the maximum-likelihood classifier.

The unsupervised (clustering) technique used in this study divides the pixels contained in a defined area into a preselected number of spectral classes. Pixels are separated into the desired number of groups (classes) based solely on the spectral distribution within the data set. Data with similar spectral responses or spectral signatures are clustered together in groups. These spectral groups are not necessarily representative of resource classes being mapped, but they do ideally represent the spectral variability within the defined area of the image.

Supervised classification techniques use training sets to define the spectral signatures of a group or class. A group of pixels (area on the image) which is considered to be representative of a class (for example, a land-use type) is selected as a training set. The range and distribution of pixel values for a given training set define the spectral signature of the class that the pixels represent. In the classification process, each pixel of interest is evaluated and then grouped into the class which has the same or a similar spectral signature, as defined by the training set representing the class.

The parallelepiped-decision function is included as hardware in some image-processing systems, thus allowing extremely fast classification. This decision function calculates the minimum and maximum pixel values in each spectral band for the pixels contained in a given training set. Using this function, a given pixel is assigned to the class represented by a training set if the pixel value for each of the spectral bands falls within the minimum and maximum values calculated for that training set. The design of this function may result in some pixels not being classified because they do not fit the range of values for any of the training sets. Conversely, if a given pixel value meets the criteria defined by more than one training set, it will be included in more than one class.

Maximum-likelihood classifiers provide one solution to the problem of overlap or exclusion of pixels resulting from the use of the parallelepiped-decision function. The maximum-likelihood technique uses the same approach

as the parallelepiped-decision function for selecting training sets to define the spectral characteristics of selected classes. However, using the maximum-likelihood classifier if a pixel to be classified does not fit directly into one class, or if it fits more than one class, the classifier assigns the pixel to the single class to which it has the greatest probability of belonging. The probabilities are calculated by comparing the mean, variance, and covariance between spectral bands for each class (training set) with the value of the pixel to be classified. Maximum-likelihood classifiers require more processing time than the parallelepiped-decision function, but they generally provide more accurate results for a detailed classification.

Digital-Image-Processing Equipment

Digital-image-processing systems generally fall into the category of either interactive or batch computer systems involving various combinations of hardware and software components. The remainder of this discussion will consider only the interactive computer systems with specific emphasis on the Image-100 System and the Interactive Digital Image Manipulation System (IDIMS).

Most interactive digital-image-processing systems can accept analog data in the form of film images, digital data on computer-compatible digital tapes, or both. Results of processing and analysis can be photographed from a television screen display or recorded on magnetic tape for later use in a film recorder, line printer, or plotter. Some systems also have the capability to produce results from the computer memory directly to a gray-level or alphanumeric printer or plotter. The Image-100 System and IDIMS have all of these capabilities.

Some of the processing and display functions which are common to both systems include:

1. Multispectral data processing and classification (three or more channels).
2. Black-and-white and color television display of multispectral data including classification results (as many as 512×512 pixels per display).
3. Functions to correct for geometric distortion in images.
4. Image-enhancement functions including:
 - a. Arithmetic manipulation of pixels (such as addition and multiplication).
 - b. Intensity transformations (such as contrast stretching).
5. Statistical analysis of data and classification results.

6. Calculation of pixel numbers per class with areal conversions (such as acres or hectares).

A brief discussion of certain capabilities and limitations of the Image-100 System and IDIMS is presented in the following paragraphs. Detailed comparative descriptions of these and other similar systems are contained in Carter, Billingsley, and Lamar (1977).

Image-100 System.--The Image-100 System is a combination hardware/software system with a number of hardwired functions. The Image-100 System will accept supplementary data, such as maps or aerial photographs, by use of a scanning television camera which converts analog signals to digital data. Digital data may then be registered and overlaid with other digital information (that is, Landsat pixels) for additional processing and analysis. At the time of this study, the Image-100 System contained a supervised classification function (parallelepiped) without a maximum-likelihood classifier. However, the Image-100 System's parallelepiped-decision function is in a solid-state form (hardwired) allowing extremely fast classification.

IDIMS.--The IDIMS is also a combination hardware/software system, but the majority of the functions are software controlled. The software implemented functions require more time to complete but they in turn allow more flexibility in their application and operation. The IDIMS can be used for unsupervised classification (clustering) and for supervised classification using a maximum-likelihood classifier. The IDIMS configuration at the time of this study did not have a scanning television camera for input of supplementary data.